A window into the early evolutionary history of Cercopithecidae: Late Miocene evidence from Chad, Central Africa

Laurent Pallas, Guillaume Daver, Hassane Mackaye, Andossa Likius, Patrick Vignaud, Franck Guy

A window into the early evolutionary history of Cercopithecidae: Late Miocene evidence from Chad, Central Africa.

Laurent Pallas[a], Guillaume Daver[a], Hassane T. Mackaye[b], Andossa Likius[b], Patrick Vignaud[a], Franck Guy[a]

[a] PALEVOPRIM: Laboratoire de Paléontologie, Evolution, Paléoécosystèmes et Paléoprimatologie; UMR CNRS 7262, Université de Poitiers, 86022 Poitiers cedex, France.

[b] Département de Paléontologie, Université de N'Djamena, BP 1117, N'Djamena, République du Tchad.

* F. Guy and G. Daver are both senior authors.

Correspondence and requests for materials should be addressed to F.G: (email: franck.guy@univ-poitiers.fr)

Author contributions: L.P., G.D. and F.G. equally contributed to designed researches; L.P., G.D. and F.G. equally contributed to the research; L.P., G.D., F.G., H.T.M., A.L. and P.V. equally contributed to analyzing the data; L.P., G.D. and F.G. equally contributed to writing the paper.

Declarations of interest: none.

Abstract

Central Africa is known as a major center of diversification for extant Old World Monkeys (OWM) and yet has a poorly documented fossil record of monkeys. Here we report a new colobine monkey (*Cercopithecoides bruneti* sp. nov.) from the Central African hominin-bearing fossiliferous area of Toros-Menalla, Chad at ca. 7 Ma. In addition to filling a gap in the spatial and temporal record of early OWM evolutionary history, we assess the ecomorphological diversity of early OWM by providing evidence on the onset of a folivorous diet and a partial reacquisition of terrestrial locomotor habits among Miocene colobines. We also support the phylogenetic affinities of the genus *Cercopithecoides* among the stem group of the extant African colobine monkeys.

Keywords: *Cercopithecoides*, Colobinae, stem Colobini, Adaptive Radiation, Ecomorphology

Introduction

With an extensive geographical distribution, a rich taxonomy and a marked ecomorphological diversity, extant Cercopithecidae (i.e., Colobinae and Cercopithecinae) represent one of the most successful adaptive radiations of Neogene primates on the African and Eurasian continents. Old World Monkeys (OWM) are known to diverge from an ancestral African stock (i.e., Victoriapithecidae) presenting dentognathic and postcranial morphologies adaptively linked to frugivory and terrestrial locomotion (Harrison, 1989; Benefit, 1993). Extant African (i.e., Colobini) and Asian (i.e., *Presbytini*) representatives of the subfamily Colobinae depart from this adaptive zone in exhibiting morphological and physiological adaptations associated with folivory and arboreal locomotion. While a rich Miocene OWM fossil record is documented in Eurasia at 8.5-6 Ma with the radiation of the putative stem colobine *Mesopithecus* spp. (Delson, 1973), the fossil record of Miocene OWM in Africa is sparse. Dating back as far as 12.5 Ma, the African cercopithecid fossil record is known from only a handful of localities mostly restricted to East (Benefit and Pickford, 1986; Leakey et al.,

2003; Hlusko, 2007; Frost et al., 2009; Gilbert et al., 2010; Nakatsukasa et al., 2010; Suwa et al., 2015) and North Africa (Delson, 1973; Benefit et al., 2008). In spite of being suggested as a cradle of diversity for extant Cercopithecidae (Böhm and Mayhew, 2005; Ting, 2008), Central Africa has provided little evidence of the early evolutionary history of OWM (Gundling and Hill, 2000). The Central African hominin-bearing fossiliferous area of Toros-Menalla (TM), Chad at ca. 7 ± 0.2 Ma (Brunet et al., 2002; Lebatard et al., 2010) has yielded colobine remains, giving us the unique opportunity to assess current hypotheses regarding the paleobiology and phylogenetic relationships of Late Miocene colobines in Africa. Particularly, the well-preserved dentognathic materials from TM fill a temporal gap between a primitive dental morphology related to frugivory (Benefit et al., 2008; Merceron et al., 2009; Rossie et al., 2013; Suwa et al., 2015; Thiery et al., 2017) and a derived dental morphology linked to a leaf-dominated diet (Gilbert et al., 2010). Moreover, the discovery of a nearly complete forelimb allows us to reconsider the emergence of terrestrial locomotor behavior among Miocene colobines (Leakey et al., 2003; Youlatos et al., 2012). In addition, the chronological setting of TM encompassed the estimated divergence times of extant crown Colobini taxa (Ting, 2008), permitting to assess hypotheses regarding the placement of the Chadian colobine among the stem or crown Colobini group (Jablonski and Frost, 2010; Frost et al., 2015). Here we describe *Cercopithecoides bruneti* sp. nov. from the Late Miocene of Central Africa, at ca. 7 Ma and provide new evidence for terrestrial locomotor habits and an increase in leaf consumption among Miocene colobines. We also provide insights into the phylogenetic affinities of the Chadian colobine, and discuss the contribution of TM to our understanding of cercopithecid evolution in light of the ecomorphological diversity of Late Miocene OWM in a previously unknown spatial and temporal setting.

Materials and methods

Material availability and imaging

All the materials described here have been collected between 2000 and 2003 by the Mission Paléoanthropologique Franco-Tchadienne (P.I. Michel Brunet) and are currently curated at the Service de Valorisation des Collections de Paléontologie (CNRD de N'Djamena). Apart from glue consolidation, the fossil material was not subjected to any modification. All the fossil material described here has been scanned at the Université de Poitiers, France. An Easy Tom XL duo μCT-scanner yielded virtual image stacks of the Chadian fossil material with resolutions ranging from 21.5µ to 45.6μ. Virtual reconstruction and visualization were obtained with the software Avizo Standard Edition.

Comparative sample

Qualitative and quantitative data for *Cercopithecoides williamsi* were gathered from µ-CT scan data provided by the Ditsong National Museum of Natural History (Plio-Pleistocene Section). Qualitative and quantitative date for all other early African colobines derived from the literature. Qualitative and quantitative data for the dentognathic fossil material of early Eurasian Colobinae (i.e., *Mesopithecus* ssp.*)* were gathered from µ-CT scans data of high quality dental casts provided by Dr. Gildas Merceron. *Mesopithecus pentelicus* postcranial data were taken directly from specimens of the Pikermian sample curated at the Museum National d'Histoire Naturelle (MNHN, France).

Postcranial and odontometric data for extant Cercopithecidae were gathered directly from specimens provided by PALEVOPRIM (Université de Poitiers, France); the Museum National d'Histoire Naturelle (MNHN, France); the Royal Museum of Central Africa (RMCA, Belgium); the Natural History Museum of Basel (NMB, Switzerland); the Anthropological Institute and

Museum, University of Zurich (AIM-UZH, Switzerland) and the Musée des Confluences, Lyon (MHNL, France). Additional odontometric data of extant Colobini were also gathered from high quality dental casts provided by Dr. Gildas Merceron.

Mandibular data of extant Colobinae were extracted from virtual specimens provided by the Smithsonian Institution (Division of Mammals, USA); Harvard University (Museum of Comparative Zoology (MCZ), USA)); the Digital Morphology Museum (Primate Research Institute, Kyoto University) and the American Museum of Natural History (Department of Anthropology, USA).

Humeral geometric cross-sectional properties were obtained on virtual specimens provided by the Harvard University (Museum of Comparative Zoology (MCZ), USA) and the Royal Museum of Central Africa (RMCA, Belgium).

Odontometric, morphological and biomechanical analyses

Odontometric

Odontometric data of the *C. bruneti* holotype and hypodigm were acquired using a Mitutoyo Digimatic caliper CD-8''CX on the original fossil material and on selected photographs obtained in Avizo Standard Edition and measured with ImageJ. Selected photographs of generated surfaces obtained in Avizo Standard Edition from µ-CT scans data of extant and extinct colobines (i.e., *C. bruneti*, *C. williamsi* and *M. pentelicus*) were used to calculate the NH/NR ratio (Benefit, 1993) as well as additional dental metrics. Odontometric data of extant Colobinae were acquired directly on specimens as well as on high quality dental casts using a Mitutoyo Digimatic caliper CD-8''CX.

Further information regarding odontometric measurement protocols, sample size, ratio formulas and references are presented in footnotes of Fig. 1, SOM Figure S2, Table 3-4 and SOM Table S2.

Mandibular

Mandibular morphometric data from *C. bruneti*, *C. williamsi* and the extant Colobinae comparative sample were obtained from selected symphyseal and corporeal cross-sections obtained via GeoMagic Studio and Avizo Standard Edition on virtual specimens. Measurements of the symphyseal and corporeal cross-sections were obtained via ImageJ.

Further information regarding mandibular morphometric measurement protocol, sample size and ratio formulas can be found in footnotes of Fig. 6 and Table 5 as well as in SOM Fig. S1.

Postcranial

Data of the *C. bruneti* postcranial specimen were acquired via a Mitutoyo Digimatic caliper CD-8''CX on the original fossil material as well as from selected photographs obtained in Avizo Standard Edition and measured in ImageJ. All data from extant Cercopithecidae were acquired directly on specimens using a Mitutoyo Digimatic caliper CD-8''CX and from digital photographs using Image J. Further information regarding samples size and measurement protocol can be found in footnotes of Figure 9 and Table 6 as well as in SOM Figure S1.

Humeral geometric cross-sectional properties were obtained via Image J's plugin Bone J on virtual specimens. In order to acquire humeral mid-diaphyseal cross-sectional properties, the virtual image stacks were first aligned at their moments of inertia and then subjected to the calculation of geometric properties. The zone of interest (*i.e.*, slice at mid-diaphysis) was subsequently obtained from the virtual image stack. Due to the lack of the humeral head of TM

266 03-034, the mid-diaphysis of the specimen was inferred at the midpoint of actual humeral length +5%.

Body mass estimation

All equationsfor estimating body mass were taken from Delson et al., 2000. Further details and extended interpretations of body mass can be found in footnotes of Table 2 and SOM Table S1.

Results

Systematic paleontology

Order **Primates** Linnaeus, 1758;

Suborder **Anthropoidea** Mivart, 1864;

Infraorder **Catarrhini** E. Geoffroy, 1812;

Superfamily **Cercopithecoidea** Gray, 1821;

Family **Cercopithecidae** Gray, 1821;

Subfamily **Colobinae** Blyth, 1863;

genus ***Cercopithecoides*** Mollet, 1947.

Type species: *Cercopithecoides williamsi* Mollet, 1947.

Generic diagnosis: As stated in Frost and Delson, 2002 "Medium to very large colobines with globular, rounded calvaria. The rostrum is short in comparison to neurocranial length, very different from *Paracolobus*, *Rhinocolobus*, *Dolichopithecus*, and *Nasalis*. It is not as short as that of *Rhinopithecus*, however. The frontal process of the zygomatic bone is narrow, unlike *Paracolobus* and *Rhinocolobus*. The inter- orbital region is broad, which is distinct from *Libypithecus*, *Rhinocolobus*, and *Nasalis*. The supraorbital tori are thick and separated from the calvaria by a deep ophryonic groove, which is distinct

181 from *Colobus*, and most species of *Presbytis* and *Trachypithecus*. The calvaria itself lacks a sagittal crest, at
182 least anteriorly, which separates it from *Paracolobus* and *Procolobus*. The P^3 lacks a protocone, which is
183 similar to modern African colobines, but different from *Libypithecus*, *Kuseracolobus*, *Paracolobus* and
184 *Rhinocolobus*. The mandibular symphysis is steep, but shallow and pierced by a median mental foramen
185 (except in *C. meaveae*), which is different from all colobines other than *Procolobus* (*Procolobus*) and
186 *Rhinocolobus* from the Turkana Basin. The mandibular corpus is shallow and thick, which contrasts greatly
187 with that of *Kuseracolobus*, *Rhinocolobus*, *Paracolobus* and to some degree *Colobus*, but is not unlike that
188 of *Procolobus* (*Piliocolobus*). The gonial region is unexpanded or expanded only a small amount. This
189 contrasts with mandibles of *Kuseracolobus*, *Rhinocolobus*, *Paracolobus mutiwa*, and *Colobus*. Associated
190 postcrania are known for *C. williamsi* from an associated skeleton from Koobi Fora (the morphology of
191 which may not be typical for the South African material, see remarks below). It is distinguished from all
192 other known colobines, except *Dolichopithecus*, in the degree of its adaptations for terrestrial habitus
193 (Birchette, 1981; 1982; Ting, 2001)."
194 On a taxonomic level, the combination of a faint P^3 protocone, a precocious and marked dental wear, an
195 orthognathic subnasal region with short premaxillae and maxillary sinuses (MS), a buttressed corpus
196 bulging below M_{1-2} as well as a symphysis with a straight, smooth and vertical labial face align the Chadian
197 cercopithecid with the East and South African genus *Cercopithecoides* (Freedman, 1957; Frost and Delson,
198 2002; McKee et al., 2011) (Table 1-2).
199 ***Cercopithecoides bruneti*** sp. nov. Holotype: TM 266 03-100, left and right hemimaxillae preserving dI^1,
200 dC^1, dP^{3-4}, C^1, P^{3-4}, M^{1-2}. Paratype: TM 266 03-034, a fragmented left and right maxilla with I^2, C^1-P^4; TM 266
201 03-099, partial mandible preserving left P_3-M_3 and associated right P_3-M_1; TM 112 00-093, partial mandible
202 preserving left P_3; TM 219 01-102, partial mandible preserving left C_1 and right I_1-M_2; TM 266 03-036, a right

partial forelimb with sub-complete humerus, ulna and radius; TM 266 03-307, a sub-complete right femur. Type locality: Locality n°266 from the fossiliferous area of Toros-Menalla, western part of the Djurab desert, northern Chad basin. Type horizon: Anthracotherid Unit. Age*:* ca. 7 ± 0.2 Ma. Etymology: In honor of Pr. Michel Brunet for his significant contribution to paleoanthropology in Central Africa. Since 1994, he has initiated, led and directed the fieldwork of the Mission Paléoanthropologique Franco-Tchadienne (MPFT) in Chad.

Specific diagnosis: A colobine of moderate size, similar in overall dental dimensions and inferred body mass to *Paracolobus enkorikae* (Lemudong'o Formation (Fm.), Kenya)*, Mesopithecus pentelicus, Libypithecus markgrafi* (Wadi Natrun Fm., Egypt)*,* colobine gen. and sp. A from Mpesida (Mpesida Beds, Tugen Hillas, Kenya) and colobine sp. B from Lower (LN) and Upper Nawata (UN) (Nawata Fm., Lothagam, Kenya). Upper dentition with moderate cusp relief and molar flare, M^2 paraloph width enlarged relative to tooth length, P^3 protocone highly reduced relative to paracone, dP^4 paraloph width enlarged relative to tooth length and marked breadth differential between P^3 and P^4. Lower dentition with a narrow P_4 crown, a marked size differential between M_1 and M_2, M_3 lacking a tuberculum sextum and possessing a bucco-lingually narrow hypoconulid relative to hypolophid breadth. Craniofacial morphology characterized by maxillary sinuses and an orthognathic sub-nasal region. Mandibular morphology characterized by a prominent inferior transverse torus (ITT), a corpus of moderate robustness with marked prominentia lateralis and a deep mandibular symphysis with a flat and vertical labial face that lacks a median mental canal.

Differential diagnosis *Cercopithecoides bruneti* specimens are larger than *Microcolobus tugenensis* (Ngorora Fm., Tugen Hills, Kenya), *Microcolobus* sp. (Nakali Fm., Baringo, Kenya) and the indeterminate small colobines from Kabasero (Ngorora Fm., Tugen Hills, Kenya), Teso Tadecho (Chorora Fm., Ethiopia),

225 Beticha (Chorora Fm., Ethiopia), Lukeino (Lukeino Fm., Tugen Hills, Kenya), Lemudong'o (Lemudong'o Fm.,
226 Kenya) and colobine sp. A from LN-UN (Nawata Fm., Lothagam, Kenya). The Chadian colobine is smaller
227 than the Miocene colobines from Menacer (Algeria) and Adu Asa (Adu Asa Fm., Ethiopia) as well as from
228 the early Pliocene *Kuseracolobus hafu*. *C. bruneti* exhibits an enlarged paraloph relative to M^2 length with a
229 crown shape ratio (CSR) matched by the small colobine from Lemudong'o (Fig. 1). *C. bruneti* further differs
230 from *M. tugenensis* by the presence of an ITT, enlarged prominentia lateralis, a marked size differential
231 between M_1 and M_2, a less developed talonid on P_3 and a narrow P_4 crown. *C. bruneti* is distinct from the
232 Kabasero colobines in having a more developed hypoconulid and a narrow hypolophid relative to M_3
233 length. Forelimb morphology of *C. bruneti* is unlike the Nakali colobine in having a reduced and straight
234 ulnar olecranon process and a short and retroflexed humeral medial epicondyle. *C. bruneti* is distinguished
235 from the Teso Tadecho colobine, *Paracolobus enkorikae*, the small Lemudong'o colobine and *L. markgrafi*
236 by having a reduced P^3 protocone. A marked breadth differential between P^3 and P^4 further differentiates
237 *C. bruneti* from *P. enkorikae*, the small colobine from Lemudong'o and *L. markgrafi*. *C. bruneti* is also
238 distinguished from the Teso Tadecho colobine by a broader P^4 crown. *C. bruneti* further differs from *P.*
239 *enkorikae* by a narrow P_4 crown, maxillary sinuses and a flat symphyseal labial face with no break in slope.
240 *C. bruneti* is morphologically distinct from *L. markgrafi* in having a narrow C^1. *C. bruneti* differs from the
241 Mpesida Beds colobine gen. and sp. A in lacking a buccally curved hypoconulid and accessory cuspules
242 between entoconid and hypoconulid and in exhibiting a broader hypolophid relative to tooth length. *C.*
243 *bruneti* differs from *Kuseracolobus aramisi* by a reduced P^3 protocone (a feature described as variable in *K.*
244 *aramisi*), an early eruption of molars relative to the anterior dentition, a marked dp^4 CSR, a moderate flare
245 on M^2 with a marked M^2 CSR (i.e., with a value > 100), a marked P^{3-4} breadth differential, a corpus with a
246 sharp inferior margin, the presence of a double mental foramen and an absence of tuberculum sextum.

247 *C. bruneti* is one of the smallest species of the East and South African genus *Cercopithecoides*, with dental
248 dimensions similar to *Cercopithecoides kerioensis, C. meavae*, *C. alemayehui* and *C. haasgati*. It differs from
249 the large taxa *C. williamsi* and *C. kimeui* in lacking a median mental canal and in possessing a gracile corpus.
250 It further differs from *C. williamsi* in possessing a shorter planum alveolare, a relatively smaller
251 hypoconulid, a superiorly placed genioglossal fossa, a less marked size differential between ITT and STT
252 (Superior Transverse Torus), a less developed humeral deltoid crest, a less developed humeral medial
253 trochlear keel and a broader zona conoidea. *C. bruneti* is distinct from *C. meavae* in having a marked
254 breadth differential between P^{3-4}, a broader dP^4, a less marked size differential between M_{1-2}, a shorter
255 humeral medial epicondyle, a less developed humeral medial trochlear keel, a less rounded radial head
256 and a gracile radial neck. *C. bruneti* also differs from *C. alemayehui* by a narrower P^3 crown and a broader
257 M^2 paraloph relative to tooth length. *C. bruneti* displays an increased breadth differential between P^{3-4}
258 relative to *C. kerioensis* (Fig. 1) and is distinguished from *C. haasgati* by a narrower P^3 crown, an elongated
259 P_4 crown and a less marked size differential between M_1 and M_2.
260 ***Description of* C. bruneti *dentognathic morphology***
261 TM 266 03-100 The type specimen TM 266 03-100 is a right and left hemimaxilla belonging to a juvenile
262 individual and preserving much of the upper postcanine dentition (Table 3, Fig. 2). Of the upper anterior
263 dentition, the dI^1 are highly worn, a small portion of the left dC^1 root is preserved and a large portion of the
264 C^1 crown remained intact in the dental crypt. The dI^1 exhibits a lingual rootward extension of enamel onto
265 the cervix and a mesiodistally compressed root unfused at its apex. The upper canine displays the features
266 characteristic of male cercopithecids (i.e., deep mesial sulcus, a sharp distal margin, a convex buccal face
267 and a mesiodistal elongation of the canine crown relative to breadth). Deciduous premolars are severely
268 worn, consistent with a J5 dental wear stage while the postcanine dentition already show an A2 wear stage

269 (Ingicco et al., 2012). This early and heavy wear of the dentition is unusual among extant colobines,
270 especially when considering the ontogenetic status of the specimen. The deciduous upper premolars
271 exhibit a large amount of flaring and a CSR consistent with a bucco-lingual enlargement of those teeth. The
272 dP^3 is bilophodont and devoid of *crista obliqua*; the dP^4 possesses a paraloph broader than the metaloph
273 and a mesial shelf longer than the distal one (SOM Table 2). M^{1-2} are in occlusion while dI^1 is still in place,
274 confirming the presence of an early eruption of M^2 relative to the anterior dentition. The permanent
275 premolars are preserved in their crypts and exhibit a characteristic colobine morphology. The P^3 crown is
276 moderately broad and exhibits heteromorphic cusps with a faint protocone, a well-developed mesiobuccal
277 flange, a paracone set distally relative to the protocone and a relatively narrow triangular mesial shelf
278 compared to a squared-shape distal shelf. The P^4 crown is broad, displays a paracone higher than a distally
279 set protocone, a high paracone relative to crown length, a high and sharp transverse loph, a marked
280 mesiobuccal flange, a slight lingual cleft and a moderate length differential between mesial and distal
281 shelves. In addition, there is a marked breadth differential between P^{3-4} (Fig. 1). The M^2s exhibit
282 qualitatively thin enamel (Fig. 2) as well as a moderate amount of flare and crown relief relative to extant
283 colobines. Note that the buccal parts of both M1 are missing as well as the hypocone of both M2 (Fig. 2).
284 M^{1-2} present deep and marked median lingual clefts, a poor development of the mesiodistal
285 developmental groove, widely spaced lophs and moderately developed shelves (SOM Table S2) that
286 support the taxonomic status of TM 266 03-100 as a colobine (Benefit, 1993). A marked buccal cingular
287 ridge is present on M^2 and a poorly developed interconulus is observed at the base of the M^1 lingual cleft. A
288 body mass of ~16.5kg is inferred from M^{1-2} mesio-distal dimensions (SOM Table S1). Considering
289 craniofacial morphology, TM 266 03-100 exhibits an orthognathic subnasal region with an anteriorly placed
290 zygomatic process which originates low on the maxilla and above M^1. This morphological pattern is seen in

291 extant juvenile Colobinae and Cercopithecini of similar dental eruption stage (Fig. 3). The nasal aperture is
292 straight in lateral view and tapers inferiorly to form an acute inferior margin in anterior view. The
293 premaxilla is reduced and gives a square aspect to the premaxillo-maxillary complex. No maxillary or
294 infraorbital fossae are observed. A large infraorbital foramen is present on the inferior portion of the orbital
295 margin of the right hemimaxilla. The hard palate extends posteriorly at the level of M^2. Maxillary sinuses
296 (MS) invade the lower portion of the maxilla, extend anteriorly at the level of M^1 and are pierced by the
297 roots of M^{1-2}.
298 TM 266 03-034 is a fragmented anterior maxilla preserving most of the adult anterior dentition (Fig. 2). I^2
299 displays a parallelogram-shaped and mesially angled crown with a poorly developed basal cingulum, a faint
300 lateral prong, a thin layer of enamel on the occlusal surface, a well-defined and horizontal cervix, a
301 markedly convex labial face and no sulcus. C^1 presents a narrow crown with a long axis obliquely oriented
302 relative to P^{3-4}, a low crown cusp with a raised cingulum on the mesial margin, a raised distal margin on the
303 talonid and a mesial groove continuing from the crown onto the roots. TM 266 03-034 exhibits a female
304 morphology with a low crowned C^1 relative to tooth length. Although fragmented, the P^3 bucco-lingual
305 dimension is in the size range of TM 266 03-100 (SOM Table S2) and is morphologically consistent with the
306 *C. bruneti* holotype in exhibiting a flange-like buccal margin and a raised paracone associated with a faint
307 and mesially offset protocone. A slight portion of the lateral margin of the right nasal aperture is preserved
308 and set vertically relative to the occlusal plane.
309
310 TM 266 03-099, TM 112 00-093 and TM 219 01-102 consist of adult mandibular remains
311 allocated to the *C. bruneti* hypodigm (Fig. 4-5).
312 TM 266 03-099 displays a wear pattern consistent with an A6 dental wear stage (Ingicco et al.,
313 2012). The P_3 crown is narrow and presents a large protoconid but no paraconid nor metaconid,

314 the mesiobuccal flange is developed, upright, and does not extend below the alveolar margin.
315 The degree of development of the P_3 flange is consistent with a male morphology. The P_4 is
316 bicuspid, lacks an entoconid and displays a protoconid broader than the distally offset
317 metaconid and an elongated crown with a moderate mesiobuccal flange. Mesial and distal
318 lophids are of nearly equal width on M_{1-2} but there is a marked size differential between M_1 and
319 M_2 (SOM Fig. S2). The trigonid basin is reduced on all molars, and the M_3 lacks a tuberculum
320 sextum but bears a buccally placed hypoconulid which is small relative to hypolophid breadth.
321 The labial symphyseal face is flat and vertical with a minute symphyseosum foramen placed at
322 its mid-height. It lacks rugosities, sub-incisal hollowing and a median mental canal (Fig. 4-5). The
323 inferior margin of the symphysis is sharp with a rugose infero-lingual portion, a developed
324 digastric spine and a poorly imprinted digastric fossa. The planum alveolare is straight and
325 extends to the mesial part of P_3. The symphysis is robust (Fig. 4-5) and presents a bulbous and
326 extensive ITT that reaches the mesial part of P_4. The infero-lingual margin of the corpus is sharp
327 and inferiorly lacks an imprinted digastric fossa at M_1 level and superiorly an inter-toral sulcus.
328 Prominentia laterales are prominent and extend anteriorly to the mesial portion of P_4. The
329 corpus is deep and bulges below M_1, the linea obliqua merges with the corpus at the level of M_{1-2}
330 contact and the extramolar sulcus is narrow.
331 TM 112 00-093 morphology is consistent with that of TM 266 03-099 in exhibiting a similar
332 symphyseal topography but with a less developed ITT extending only to the level of P_3 and a less
333 acute symphyseal inferior margin. The planum alveolare is slightly concave and the STT
334 overhangs a shallow genioglossal fossa. The corpus morphology is also consistent with TM 266
335 03-099 but exhibits a marked imprinting of the digastric fossa and submandibular fossa,

336 respectively below P_4-M_1 and M_{2-3}. Of the entire dental row, only the P_3 crown is preserved. The
337 mesiobuccal flange is short and in accordance with a female morphology. The incisor row is
338 narrow. The base of the M_3 crown tapers distally.
339 TM 219 01-102 is a fragmented mandible preserving the symphysis and hints of the superior
340 portion of the right and left corpus. TM 219 01-102 exhibits peg-like incisors with poorly
341 developed cingulum and a narrow incisal row. Canines are robust, labially recurved, and present
342 an extensive talonid devoid of any tubercles. The canine root bears a faint mesial groove. The
343 inferior margin of the symphysis is eroded but the toral morphology is clearly colobine-like with
344 an extensive and bulbous ITT reaching the mesial part of M_1. The symphysis is vertical, and a
345 slight hint of the linea obliqua is preserved on the upper part of the corpus at the level of M_2.
346 Canine dimensions and morphology are consistent with identification as a male. In addition,
347 dental and mandibular dimensions of TM 219 01-102 are congruent with those of TM 266 03-
348 034 (Tables 4-5).
349 Body masses inferred from dental dimensions ranged from ~ 8.45kg for TM 112 00-093 to ~
350 13.3kg and ~14.4kg (using equations from Delson et al., 2000), respectively for TM 219 01-102
351 and TM 266 03-099 (SOM Table S1).
352
353 ***Comparative aspect of* C. bruneti *dentognathic anatomy***

354 The *C. bruneti* dP^4 possess a paraloph broader than the metaloph (SOM Table S2), a
355 characteristic variable among Cercopithecoidea but mostly observed on Victoriapithecidae and
356 Cercopithecinae (Benefit, 1994). Nevertheless, the absence of a crista obliqua, the bilophodont
357 state of dP^{3-4} and the marked dP^4 mesial shelf length relative to the distal one clearly aligns *C.*

358 *bruneti* with crown cercopithecids (Benefit, 1994). The dP^4 CSR is consistent with an
359 enlargement of the tooth, similar to victoriapithecids but also to the putative colobine dP^4 from
360 Menacer (SOM Fig. S2). Furthermore, the early eruption of M^2 relative to the anterior dentition
361 observed in *C. bruneti* is typical of Colobinae (Harvati and Frost, 2007). Although an early molar
362 eruption relative to anterior dentition was previously documented in *M. pentelicus*, the extreme
363 condition of the early eruption of M^2 relative to I^1 observed in *C. bruneti* was previously
364 unknown among fossil colobines whereas it is documented either as a variant (e.g *Colobus*
365 *angolensis*) or as a constant (*e.g Presbytis* spp.) among extant Colobinae (Harvati and Frost,
366 2007). *C. bruneti* upper molar morphology is similar to those of early Eurasian as well as North
367 and East African colobines in exhibiting a basal flaring associated with a lack of sharp shearing
368 crests (Benefit and Pickford, 1986; Rossie et al., 2013; Suwa et al., 2015). Even slightly worn, a
369 quantification of *C. bruneti* left M^2 occlusal relief (i.e., NH/NR ratio, Fig. 1) yields a value higher
370 than those observed among the penecontemporaneous Eurasian colobine *M. pentelicus* and the
371 North African colobines from Menacer and As Sahabi (Delson, 1973; Benefit et al., 2008). *C.*
372 *bruneti* subnasal morphology is consistent with the poor maxillary projection observed in
373 *Cercopithecoides* spp. and *Kuseracolobus* spp. The deep and slender corpus as well as the deep
374 symphysis of *C. bruneti* is similar to the early Pliocene *C. kerioensis* (Leakey et al., 2003). The
375 Chadian *Cercopithecoides* further shares with *C. kerioensis* and *C. meavae* a moderate breadth
376 of the M_3 hypolophid relative to tooth length and an absence of a median mental canal. *C.*
377 *bruneti* is similar to the South African *C. williamsi* sample in exhibiting a marked P^{3-4} breadth
378 differential (Fig. 1,3) and a marked M_{1-2} size differential (SOM Fig. S2). The enlargement and the
379 square aspect of the *C. bruneti* upper second molar are also consistent with the South African

Cercopithecoides sample (i.e., *C. williamsi* and *C. haasgati*) (Fig. 1,3). Relative to extant colobines, *C. bruneti* dentognathic morphology is consistent with a Colobini morphology. Indeed, a narrow P^3 crown with heteromorphic cusps (Swindler and Orlosky, 1974), a height differential between lingual and buccal P^4 cusp (Gilbert et al., 2010), a distally offset P_4 metaconid (Swindler and Orlosky, 1974), a broad P_4 protoconid relative to metaconid (Swindler and Orlosky, 1974), a narrow P_4 crown, an elongated C^1 (Pan, 2006) and a poorly developed (i.e., *Colobus*-like) digastric fossa (Groves, 2007) aligns *C. bruneti* with the extant Colobini (Fig. 3). In spite of morphological affinities with the African colobine tribe, *C. bruneti* lacks the long and steeply inclined planum alveolare, the inferiorly placed genioglossal fossa and the diminutive ITT seen among several taxa of *Colobus* (Fig. 5-6). *C. bruneti* symphyseal topography is most consistent with the morphology exhibited by *Piliocolobus* but it does not exhibit the marked dental occlusal relief seen in the extant genus (Fig. 5-6).

Description of* C. bruneti *postcranial morphology

A sub-complete right forelimb (i.e., TM 266 03-036) composed of humerus, radius and ulna as well as a partial femur (i.e., TM 266 03-307) are here included in the *C. bruneti* hypodigm (Fig. 7). Collected from the same locality, it is parsimonious to assume that the fore- and hindlimbs come from the same taxon (i.e., *C. bruneti*). Joint congruency supports the hypothesis of the forelimb elements belonging to the same specimen.

<u>TM 266 03-036</u> The postero-distal portion of the humeral head is preserved and is flanked by well-defined distal margin of the greater and lesser tuberosities. In posterior view, the medial part of the surgical neck is markedly concave and accommodates the insertion of the

401 coracobrachialis profundus muscle. The humeral proximal diaphysis is fractured in its proximal
402 and distal portion. It is surrounded by sharp crista tuberculi majoris and crista tuberculi minoris.
403 Those crests are poorly developed and accommodate proximally set attachment sites for teres
404 major and pectoralis major muscles. The posterior aspect of the proximal diaphysis is salient
405 and bears moderate sites of attachment for the lateral head of the triceps brachii muscle. The
406 deltoid tuberosity is flat, poorly developed, and does not extend below mid-diaphysis. The
407 humeral diaphysis is gracile and elliptical in cross-section at mid-diaphysis, with a long-axis
408 running anterolateral-to-posteromedially. The humeral shaft is straight in the anteroposterior
409 plane but curved medially in the mediolateral plane. The posterior aspect of the distal portion of
410 the diaphysis is flattened and exhibits a poorly developed lateral supracondylar ridge. The distal
411 epiphysis is fractured and separated from the humeral shaft. Most of the humeral trochlea and
412 zona conoidea are preserved (Fig. 7). The antero-proximal part and a slight hint of the proximo-
413 lateral portion of the capitulum are preserved. The anterior aspect of the distal epiphysis is
414 characterized by a wide and deep radial fossa, a shallow and poorly delineated coronoid fossa, a
415 moderate-sized trochlea, a moderately developed medial trochlear keel compared to
416 cercopithecins that is set obliquely relative to the long-axis of the shaft, a well-defined anterior
417 margin of the medial trochlear keel, a faint lateral trochlear keel and a large zona conoidea (Fig.
418 7)**.** The posterior aspect of the distal epiphysis exhibits a deep and oval-shaped olecranon fossa
419 that presents a septal aperture, a moderate breadth differential between its lateral and medial
420 pillar, a short and retroflexed medial epicondyle and a salient posterior margin of the lateral
421 pillar of the olecranon fossa.

422 The cresting of the proximal portion of the ulnar olecranon process is damaged (Fig. 7). The

olecranon process is short and aligned with the long axis of the diaphysis. The posterior margin of the proximal epiphysis is slightly convex. The anconeal process is short and does not project markedly anteriorly. Although eroded, the proximal margin of the anconeal process is asymmetric, with a proximal projection of its lateral margin. The ulnar sigmoid notch is fractured at its mid-height. The ulnar trochlear surface is poorly waisted and congruent with the moderate enlargement of the humeral trochlea. The postero-medial portion and the most anterior portion of the coronoid process is missing as is the postero-lateral portion of the radial notch. The anterior margin of the coronoid process is wide and is antero-distally slanted, consistent with a shallow humeral coronoid fossa. The radial notch is expanded, presents a waisting between its anterior and posterior facet and bears a lateral margin oriented posteriorly. The medial face of the proximal epiphysis is fractured longitudinally but exhibits a deep and wide insertion surface for the flexor digitorum profundus muscle that extends distally through the proximal part of the diaphysis. The ulnar diaphysis is fractured in its mid- and distal portion, resulting in separate fitting parts. The proximal portion of the diaphysis exhibits a raised supinator crest that borders a large insertion surface for the supinator muscle. The diaphysis is gracile and straight in lateral view. A raised pronator ridge is present on the distal portion of the diaphysis. The distal epiphysis is broken away.

The radius preserves the damaged proximal half. Only the antero-lateral portion of the radial head is missing (Fig. 7). The radial head is elliptical with the long-axis running antero-posteriorly. The articular fovea of the radial head is placed posteriorly and is bordered anteriorly by a wide peripheral articular surface and posteriorly by a proximally-raised margin. The radial head is strongly tilted in medio-lateral view. The neck is short, gracile, and bears a marked bicipital

445 tuberosity divided in two components by a deep sulcus. The medial margin of the proximal
446 portion of the diaphysis is slightly concave and exhibits a faint interosseous crest whereas the
447 lateral margin bears signs of rugosities for the supinator muscle.

448 TM 266 03-307 is a right femur with a damaged proximal epiphysis preserving the femoral neck,
449 the postero-proximal aspect of the greater trochanter, a slight hint of the proximal portion of
450 the intertrochanteric crest and the medial portion of the lesser trochanter. The distal third is
451 broken away (Fig. 7). The neck is antero-posteriorly compressed, bears no grooving for the
452 obturator externus tendon, forms an obtuse neck-shaft angle with the femoral shaft and is
453 poorly anteverted. The cortical bone distribution of the femoral neck is asymmetric with a
454 cortical bone distribution skewed toward the inferior margin of the neck, as in most extant
455 cercopithecids (Rafferty, 1998). The trochanteric fossa is rounded, shallow and does not extend
456 distally below the insertion for quadratus femoris. The shaft is robust and slightly bowed
457 anteriorly. The medial margin of the lesser trochanter is salient and projects postero-medially.
458 Inferiorly to the lesser trochanter is a rugose zone for the pectineal line and gluteal tuberosity.
459 Although fragmented, TM 266 03-307 is here included in the *C. bruneti* hypodigm based both on
460 its estimated body mass (SOM Table S1), which is consistent with values obtained from dental
461 dimensions, and on its provenance from the *C. bruneti* type locality (i.e., locality n°266).

462 ***Comparative anatomy and functional morphology of* C. bruneti *postcranial anatomy***

463 *C. bruneti* upper limb morphology presents clear colobine affinities in exhibiting a
464 prominent zona conoidea (Frost and Delson, 2002), a marked breadth differential between the
465 lateral and medial pillar of the olecranon fossa, an extensive ulnar insertion site for flexor

digitorum profundus (Krentz, 1993; DeSilva et al., 2013), a marked asymmetry of the peripheral articular surface of the radial head (Nakatsukasa et al., 2010) and a poorly defined interosseous crest on the radius (DeSilva et al., 2013). Considering humeral morphology, *C. bruneti* is similar to *C. williamsi*, *C. kimeui* and *C. meavae* in exhibiting a retroflexed medial epicondyle and a deep distal articular surface antero-posteriorly (i.e., *HDB* variable in Table 6) (Frost and Delson, 2002; Jablonski and Leakey, 2008). An abbreviated and retroflexed medial epicondyle has been linked to terrestrial locomotor behavior and particularly to stability enhancement of the humero-ulnar joint in pronated position (Jolly, 1967; Birchette, 1982). A moderate extension of the deltoid tuberosity and a proximal insertion of the teres major and pectoralis major illustrate an enhancement of rapid flexion/adduction of the *C. bruneti* elbow. The Chadian colobine exhibits an elliptical cross-section of the humeral mid-diaphysis, consistent with a structural adaptation related to stress dissipation of mechanical loadings engendered during terrestrial locomotor behavior (Fig. 9) (Carlson et al., 2011; Patel et al., 2013). Although structurally adapted to withstand mechanical stress and rapid flexion/extension in a terrestrial context, the functionally mosaic humeral morphology of *C. bruneti* exhibits characters reminiscent of arboreal locomotor habits. The enlargement of the humeral trochlea of *C. bruneti* is moderate, translating a weight-bearing function to the humero-ulnar joint as in extant arboreal Colobinae (Birchette, 1982). Although marked relative to extant Colobinae (Fig. 8), the development of the medial trochlear keel of *C. bruneti* is moderate relative to *C. williamsi* and *C. meavae* and reflects a humero-ulnar joint poorly adapted to restrict medial movement as occurred during leaping and/or terrestrial activities (Fig. 9) (Birchette, 1982; Harrison, 1989; Frost and Delson, 2002). The humeral shaft of *C. bruneti* is gracile and accords well with generating low reaction forces and an adaptation to

compliant substrate, as found in an arboreal context (Nakatsukasa, 1994). The insertion for the coracobrachialis profundus muscle is depressed and the insertion for the flexor digitorum profundus muscle on the ulna is marked and extensive, as in arboreal cercopithecids (Krentz, 1993). Relative to ulnar morphology, the olecranon process of *C. bruneti* is short and, coupled with a deep humeral olecranon fossa, reflects an important degree of elbow extension. The olecranon process is straight and not consistent with the anteflexed olecranon of arboreal colobines (Fig. 8) nor with the retroflexed olecranon of highly terrestrial Cercopithecinae (Birchette, 1982). In addition, the straight ulnar shaft contrasts with the posteriorly convex shaft of arboreal colobines (Fig.e 8) (Birchette, 1982). Consistent with the previously inferred weight-bearing function of the humero-ulnar joint*, C. bruneti* exhibits an enlarged humeral articular facet of the ulnar sigmoid notch (Table 6). A short anconeal process and a distally slanted coronoid process confirm the presence of a poorly stabilized humero-ulnar joint in *C. bruneti*. This flexibility of the elbow joint is consistent with an arboreal component in the locomotor behavior of the Chadian colobine. In accordance with the humeral morphology, the ulnar shaft is gracile. A marked elliptical radial head is observed in both extant *Colobus* and *C. bruneti* (Birchette, 1982). With a marked proximal projection of its posterior margin and a strong medial tilt, the radial head of *C. bruneti* is consistent with a reinforcement of the humero-radial joint in pronated position (Rose, 1988). The radial neck of *C. bruneti* is gracile and confirms the patterns of a poorly buttressed brachium and antebrachium. Considering femoral morphology, the neck-shaft angle of *C. bruneti* is obtuse, contrasting with the acute angle seen among hyper-terrestrial cercopithecids and reflecting an increase in hindlimb range of motion (Bacon, 2001; Frost).

Discussion

Cercopithecoides bruneti sp. nov. from the Late Miocene of Central Africa, Chad adds to the antiquity and to the extensive geographical range of the genus *Cercopithecoides*. The mandibular morphology of *C. bruneti* corroborates the presence of a relatively deep and slender corpus among early representatives of this genus (Fig. 4) (Leakey et al., 2003; Jablonski and Frost, 2010). It also documents a departure from the cercopithecine-like symphyseal topography documented in Miocene East African stem Colobinae (Benefit and Pickford, 1986) and brings evidence of a diversity in mandibular morphology among *Cercopithecoides*. Discrepancies in corporeal and symphyseal cross-sectional geometry and morphology further inform us on divergent structural adaptations to withstand at least different stress and loading regimes during feeding behavior (Ross et al., 2012). The relationships between diet, feeding behavior and mandibular morphology are not straightforward among primates (Daegling and McGraw, 2001; Daegling and Grine, 2017), blurring the ecomorphological signal inferred from corporeal and symphyseal morphology among early and late representatives of *Cercopithecoides* taxa. A frugivorous component was identified in the *C. williamsi* diet through Dental Microwear Textural Analysis (DMTA) (Williams and Geissler, 2014), and several proxies point to a fruit-dominated diet among Eurasian and several Late Miocene early colobines (Merceron et al., 2009; Rossie et al., 2013; Thiery et al., 2017). In contrast, the East African Miocene colobines from Lukeino Fm. and Mpesida Beds, respectively at ca. 5.7 and 6.37 Ma,

531 bear qualitative and quantitative (i.e., NH/NR) dental morphological hallmarks of adaptation to
532 a leaf-dominated diet (Gilbert et al., 2010). *C. bruneti* occlusal relief is moderate relative to
533 extant colobines but stands apart from the cercopithecine-like occlusal relief documented in
534 North African (Benefit et al., 2008) and Eurasian Miocene colobines (Fig. 1). Accordingly, *C.*
535 *bruneti* dental morphology provides evidence of an increase in occlusal relief and thus supports
536 an increase in leaf consumption at ca. 7 Ma among African colobines relative to
537 penecontemporaneous early African and Eurasian colobines. Subsequent adaptation to the
538 consumption of abrasive food items had been postulated in regard to the severe degree of
539 dental attrition wear stages observed among several *Cercopithecoides* taxa (Szalay and Delson,
540 1979; Jablonski and Frost, 2010). *C. bruneti* provides the earliest evidence of this peculiar dental
541 wear pattern which may be linked to grit transport due to the onset of the Sahara Desert in
542 Central Africa at ca. 7 Ma (Schuster, 2006).
543 The associated colobine postcranial remains from Nakali shed light on arboreal locomotor
544 behavior among Late Miocene African stem Colobinae (Fig. 8) (Nakatsukasa et al., 2010).
545 Further evidence of arboreality was inferred among several groups of early colobine postcranial
546 remains from other Miocene East African localities (Hlusko, 2007; Gilbert et al., 2010).
547 Contrasting with a plesiomorphic arboreal postcranial bauplan, the radiation of the Plio-
548 Pleistocene *Cercopithecoides* taxa has been associated with locomotor behavior that includes
549 moderate to marked terrestrial locomotor habits (Jablonski and Leakey, 2008). Morpho-
550 functional adaptation to terrestrial locomotor behavior is inferred among Eurasian Miocene
551 colobines (Fig. 8) (Youlatos et al., 2012; Youlatos and Koufos, 2010) but tenuous evidence of
552 terrestriality was postulated from fragmentary and isolated Miocene colobine forelimb remains

553 from East Africa (Leakey et al., 2003). A nearly complete forelimb attributed here to *C. bruneti*
554 firmly demonstrates a partial reacquisition of terrestrial locomotor behavior among colobines as
555 early as the Late Miocene (Fig. 8-9) and confirms the autapomorphic condition of terrestrial
556 habits in the locomotor behavior of the genus *Cercopithecoides*. Additionally, the Chadian
557 colobine documents a morpho-functional trade-off typical of *Cercopithecoides*, with an elbow
558 joint adapted to withstand stress engendered by terrestrial locomotor habits and to promote
559 joint flexibility during foraging and frequent arboreal locomotor habits (Jablonski and Leakey,
560 2008). In addition to shedding light on the locomotor diversity of early African colobines, *C.*
561 *bruneti* also establilshes the presence of an extreme variant of early molar eruption pattern
562 among Late Miocene African colobines and confirms the diversity of dental eruption pattern
563 inferred among early colobines (Harvati and Frost, 2007).
564 Toros-Menalla is similar to other East African Miocene cercopithecid-bearing localities in
565 exhibiting an abundance of Colobinae relative to Cercopithecinae (Harrison, 2011). It also brings
566 evidence for a substantial ecomorphological diversity among Miocene colobines, giving support
567 to the hypothesis of a short-fused model of the adaptive radiation of Colobinae (Frost et al.,
568 2009). The affinity of the East African *C. williamsi* with the tribe Colobini was recently reinforced
569 by the demonstration of its marked pollical reduction (Frost et al., 2015). However, the affinity
570 of the genus *Cercopithecoides* with crown or stem Colobini remains unclear. Fragmentary
571 remains from an indeterminate colobine from the Lukeino Fm. demonstrates the presence of a
572 synapomorphic Colobini astragalar morphology at ca. 6.1 Ma (Gilbert et al., 2010). Unlike the
573 colobine gen. and sp. B from Lukeino Fm., no clear synapomorphic postcranial characters permit
574 to assign *C. bruneti* within the Colobini crown group. However, the molecularly estimated

575 divergence times of extant Colobini taxa (i.e., 8-6 Ma) is clearly in the time range spanned by *C.*
576 *bruneti* (Ting, 2008). On one hand, the Chadian colobine exhibits clear dental and mandibular
577 morphological affinities with the African tribe (Fig. 3, 5). On the other hand, it retains
578 plesiomorphic features observed among morphologically conservative Miocene colobines (i.e.,
579 square molars, moderate occlusal relief and MS) (Fig. 3). Additionally, the temporal setting of *C.*
580 *bruneti* and its phenetic affinities with the early Pliocene *C. kerioensis* are in favor of its basal
581 position in the *Cercopithecoides* lineage. Altogether, *C. bruneti* supports a placement of the
582 genus *Cercopithecoides* among the stem (rather than crown) Colobini group.

583 **Summary and conclusions**

584 The newly described postcranial and dentognathic fossil cercopithecid material from the Late
585 Miocene hominin-bearing fossiliferous area of Toros-Menalla sheds light on a previously
586 unknown spatial setting during a poorly sampled, yet critical, period of the adaptive radiation of
587 colobine monkeys in Africa.

588 We demonstrate the oldest occurrence of a speciose early colobine genus previously and
589 securely known only from Plio-Pleistocene deposits of eastern and southern Africa. In addition
590 to further documenting the morphological diversity of *Cercopithecoides*, *C. bruneti* supports the
591 presence of gracile mandibular morphology as well as the autapomorphic condition of
592 terrestrial locomotor habits among early representatives of its genus. While phenetic affinities
593 of *Cercopithecoides* with the Colobini crown group are corroborated, in-depth analysis of the
594 dentognathic morphology of *C. bruneti* underlined its basal position by revealing its
595 morphological departure from the mandibular and dental anatomy of extant African colobines,

596 lending further support to a phylogenetic placement of *Cercopithecoides* into the stem Colobini
597 group.
598 As an anatomical hallmark of extant colobines, the emergence of a folivorous dental
599 morphology is of prime interest in the understanding of the colobine adaptive radiation. On this
600 aspect, *C. bruneti* departs from the cercopithecine-like occlusal relief and the subsequently
601 inferred frugivory documented among penecontemporaneous colobines, bringing evidence of
602 an increase in leaf consumption among African Miocene colobines. Similarly, we demonstrate
603 the presence of a terrestrial signal in the *C. bruneti* postcranial morphology, confirming the
604 alteration of the colobine postcranial arboreal bauplan as early as 7 Ma in Africa.
605 By providing evidence of substantial ecomorphological diversity among Miocene colobines, we
606 highlight the role of Central Africa not only in the radiation of extant cercopithecids but also in
607 the early evolutionary history of those widespread primates.
608

609 **Acknowledgements**
610 We are grateful to the Chadian authorities and to the Ministère en charge de l'Enseignement
611 Supérieur et de la Recherche, N'Djamena (CNRD ex-CNAR and Université de N'Djamena), to all
612 the members of the field surveys and excavations lead by the MPFT (P.I. M. Brunet) and to the
613 Ambassade de France (Commission des Fouilles, Paris et Ambassade de France à N'Djamena).
614 We acknowledged the contribution of M. Adoum, D. Merci and Dr. C. D. Nekoulnang. We thank
615 S. Riffaut, X. Valentin, G. Renaud, M. Pourade, Dr. A. Mazurier, J. Surault and A. Walker for
616 technical support and administrative guidance. We are grateful to Dr. G. Merceron and Dr. G.
617 Thiery for fruitful scientific discussion. We thank the Smithsonian's Division of Mammals (Dr.

618 Kristofer Helgen) and Human Origins Program (Dr. Matt Tocheri) for the scans of USNM
619 specimens used in this research. These scans were acquired through the generous support of
620 the Smithsonian 2.0 Fund and the Smithsonian's Collections Care and Preservation Fund. We
621 also thank the Museum of Comparative Zoology of the Harvard University, Lynn Lucas and Lynn
622 Copes as well as the Wenner Gren Foundation for providing access to their virtual data,
623 deposited on www.MorphoSource.org, Duke University. We are grateful to Dr. Eric Delson and
624 the AMNH Department of Mammalogy for providing access to their data, the collection of which
625 was funded by AMNH and NYCEP and deposited on www.MorphoSource.org, Duke University.
626 We also express gratitude to Dr. Justin W. Adams who collaborated with the Plio-Pleistocene
627 Section of the Ditsong National Museum of Natural History to provide us access to these data
628 originally appearing in (Adams et al., 2015) the collection of which was funded by the
629 Department of Anatomy and Developmental Biology, Monash University and deposited on
630 www.MorphoSource.org, Duke University. We thank Dr. Emmanuel Gilissen and Dr. Walter
631 Coudyzer for giving us access to the collection of the Royal Museum of Central Africa (Tervuren,
632 Belgium) and to the imagery facilities of the Université Catholique de Louvain. We
633 acknowledged the Mammalian Crania Photographic Archive Second Edition (MCPA2) of the
634 Dokkyo Medial University (http://1kai.dokkyomed.ac.jp/mammal/en/mammal.html) for the use
635 of juvenile Colobini photographs. We are grateful to Jacques Cuisin (MNHN, France), Dr. Marcia
636 Ponce de Leon (AIM-UZH), Dr. Loïc Costeur and Florian Dammeyer (NMB) and Dr. Didier Berthet
637 (MHNL) for access to specimens under their care. We also thank Associate Editor M. Tallman
638 and reviewers E. Delson and two anonymous others for their comments, which helped to
639 improve our manuscript.

640

641 **References**

642 Adams, J.W., Olah, A., McCurry, M.R., Potze, S., 2015. Surface model and tomographic archive of
643 fossil primate and other mammal holotype and paratype specimens of the Ditsong National
644 Museum of Natural History, Pretoria, South Africa. PLOS ONE. 10, e0139800.

645

646 Bacon, A.-M., 2001. La locomotion des primates du Miocène d'Afrique et d'Europe : Analyse
647 fonctionnelle des os longs du membre pelvien et systematique. Cahiers de Paléoanthropologie.
648 CNRS Editions, Paris.

649

650 Benefit, B.K., 1993. The permanent dentition and phylogenetic position of *Victoriapithecus* from
651 Maboko Island, Kenya. Journal of Human Evolution. 25, 83–172.

652

653 Benefit, B.R., 1994. Phylogenetic, paleodemographic, and taphonomic implications of
654 *Victoriapithecus* deciduous teeth from Maboko, Kenva. American Journal of Physical
655 Anthropology. 95, 277–331.

656

657 Benefit, B.R., McCrossin, M., Boaz, N.T., Paris, P., 2008. New Fossil Cercopithecoids from the
658 Late Miocene of As Sahabi, Libya. Garyounis Scienfic Bulletin. 265–282.

659

660 Benefit, B.R., Pickford, M., 1986. Miocene fossil Cercopithecoids from Kenya. American Journal
661 of Physical Anthropology. 69, 441–464.

Birchette, M.G., 1982. The postcranial skeleton of *Paracolobus chemeroni*. Ph.D. Dissertation, Harvard University.

Böhm, M., Mayhew, P.J., 2005. Historical biogeography and the evolution of the latitudinal gradient of species richness in the Papionini (Primata: Cercopithecidae): Evolution of diversity gradients. Biological Journal of the Linnean Society. 85, 235–246.

Brunet, M., Guy, F., Pilbeam, D., Mackaye, H.T., Likius, A., Ahounta, D., Beauvilain, A., Blondel, C., Bocherens, H., Boisserie, J.-R., De Bonis, L., Coppens, Y., Dejax, J., Denys, C., Duringer, P., Eisenmann, V., Fanone, G., Fronty, P., Geraads, D., Lehmann, T., Lihoreau, F., Louchart, A., Mahamat, A., Merceron, G., Mouchelin, G., Otero, O., Campomanes, P.P., De Leon, M.P., Rage, J.-C., Sapanet, M., Schuster, M., Sudre, J., Tassy, P., Valentin, X., Vignaud, P., Viriot, L., Zazzo, A., Zollikofer, C., 2002. A new hominid from the Upper Miocene of Chad, Central Africa. Nature. 418, 145–151.

Carlson, K.J., Wrangham, R.W., Muller, M.N., Sumner, D.R., Morbeck, M.E., Nishida, T., Yamanaka, A., Boesch, C., 2011. Comparisons of limb structural properties in free-ranging chimpanzees from Kibale, Gombe, Mahale, and Taï Communities. In: D'Août, K., Vereecke, E.E. (Eds.), Primate Locomotion. Springer New York, New York, NY, pp. 155–182.

Daegling, D.J., Grine, F.E., 2017. Feeding behavior and diet in *Paranthropus boisei*: The limits of

functional inference from the mandible. In: Marom, A., Hovers, E. (Eds.), Human Paleontology and Prehistory. Springer International Publishing, Cham, pp. 109–125.

Daegling, D.J., McGraw, S.W., 2001. Feeding, diet, and jaw form in west african *Colobus* and *Procolobus*. International Journal of Primatology. 22, 1033–1055.

Delson, E., 1973. Fossil colobine monkeys of the circum-Mediterranean region and the evolutionary history of the Cercopithecidae (Primates, Mammalia). Ph.D. Dissertation, Columbia University.

Delson, E., Terranova, C.J., Jungers, W.L., Sargis, E.J., Jablonski, N.J., Dechow, P.C., 2000. Body mass in Cercopithecidae (Primates, Mammalia) : Estimation and scaling in extinct and extant taxa. *Anthr. Papers Am. Mus. Nat. Hist.* 83, 1-159.

DeSilva, J.M., Steininger, C.M., Patel, B.A., 2013. Cercopithecoid primate postcranial fossils from Cooper's D, South Africa. Geobios. 46, 381–394.

Freedman, L., 1957. The fossil Cercopithecoïdea of South Africa. Annals of the Transvaal Museum. 23, 121–262.

Frost, S.R., 2001. Fossil Cercopithecidae of the Afar Depression, Ethiopia: species systematics and comparison to the Turkana Basin. Ph.D. Dissertation, City University of New York.

706

707 Frost, S.R., Delson, E., 2002. Fossil Cercopithecidae from the Hadar Formation and surrounding
708 areas of the Afar Depression, Ethiopia. Journal of Human Evolution. 43, 687–748.

709

710 Frost, S.R., Gilbert, C.C., Pugh, K.D., Guthrie, E.H., Delson, E., 2015. The Hand of *Cercopithecoides*
711 *williamsi* (Mammalia, Primates): Earliestevidence for thumb reduction among Colobine
712 monkeys. PLOS ONE. 10, e0125030.

713

714 Frost, S.R., Haile-Selassie, Y., Hlusko, L.J., 2009. Cercopithecidae. In: Haile-Selassie, Y.,
715 WoldeGabriel, G. (Eds.), *Ardipithecus kadabba* Late Miocene Evidence from the Middle Awash,
716 Ethiopia, The Middle Awash Series. University of California Press, Berkeley, pp. 135–158.

717

718 Frost, S.R., Jablonski, N.G., Haile-Selassie, Y., 2014. Early Pliocene Cercopithecidae from
719 Woranso-Mille (Central Afar, Ethiopia) and the origins of the *Theropithecus oswaldi* lineage.
720 Journal of Human Evolution. 76, 39–53.

721

722 Frost, S.R., Plummer, T., Bishop, L.C., Ditchfield, P., Ferraro, J., Hicks, J., 2003. Partial cranium of
723 *Cercopithecoides kimeui* Leakey, 1982 from Rawi Gully, southwestern Kenya. American Journal
724 of Physical Anthropology. 122, 191–199.

725

726 Gilbert, C.C., Goble, E.D., Hill, A., 2010. Miocene Cercopithecoidea from the Tugen Hills, Kenya.
727 Journal of Human Evolution. 59, 465–483.

728

729 Gilbert, W.H., Frost, S.R., 2008. Cercopithecidae. In: Gilbert, W.H., Asfaw, B. (Eds.), *Homo*
730 *erectus*: Pleistocene Evidence from the Middle Awash, Ethiopia, The Middle Awash Series.
731 University of California Press, Berkeley, pp. 115–132.

732

733 Groves, C.P., 2007. The taxonomic diversity of the Colobinae of Africa. Journal of
734 Anthropological Sciences. 85, 7–34.

735

736 Gundling, T., Hill, A., 2000. Geological context of fossil Cercopithecoidea from eastern Africa. In:
737 Whitehead, P.F., Jolly, C.J. (Eds.), Old World Monkeys. Cambridge University Press, Cambridge,
738 pp. 180–213.

739

740 Harrison, T., 1989. New postcranial remains of *Victoriapithecus* from the middle Miocene of
741 Kenya. Journal of Human Evolution. 18, 3–54.

742

743 Harrison, T.H., 2011. Cercopithecids (Cercopithecidae, Primates). In: Harrison, T. (Ed.),
744 Paleontology and Geology of Laetoli: Human Evolution in Context. Vol.2 Fossil Hominins and the
745 Associated Fauna. Vertebrate Paleobiology and Paleoanthropology Series. Springer, Dordrecht,
746 pp. 83–139.

747

748 Harvati, K., Frost, S.R., 2007. Dental eruption sequences in fossil colobines and the evolution of
749 primate life histories. International Journal of Primatology. 28, 705–728.

Hlusko, L.J., 2006. A new large Pliocene colobine species (Mammalia: Primates) from Asa Issie, Ethiopia. Geobios. 39, 57–69.

Hlusko, L.J., 2007. A new Late Miocene species of *Paracolobus* and other Cercopithecoidea (Mammalia: Primates) fossils from Lemudong'o, Kenya. Kirtlandia, The Cleveland Museum of Natural History. 72–85.

Ingicco, T., Moigne, A.-M., Gommery, D., 2012. A deciduous and permanent dental wear stage system for assessing the age of *Trachypithecus sp.* specimens (Colobinae, Primates). Journal of Archaeological Science. 39, 421–427.

Jablonski, N.J., Frost, S.R., 2010. Cercopithecoidea. In: Werdelin, L., Sanders, W. (Eds.), Cenozoic Mammals of Africa. University of California Press, Berkeley, pp. 393-428.

Jablonski, N.J., Leakey, M.G., 2008. Systematic paleontology of the large colobines. In: Jablonski, N.G., Leakey, M.G. (Eds.), Volume 6 The Fossil Monkeys, Koobi Fora Research Project. California Academy of Sciences, Golden Gate Park, San Francisco, California, pp. 31-103.

Jolly, C., 1967. The evolution of the baboons. In: Vagtborg, H. (Ed.), The Baboon in Medical Research. Volume II: Proceedings of the First International Symposium on the Baboon and Its Use as an Experimental Animal. University of Texas Press, Austin, pp. 23–50.

772

773 Krentz, H.B., 1993. Postcranial anatomy of extant and extinct species of *Theropithecus*. In:
774 Jablonski, N.G. (Ed.), *Theropithecus*: The Rise and Fall of a Primate Genus. Cambridge University
775 Press, pp. 383–425.
776
777 Leakey, M.G., Teaford, M.F., Ward, C.V., 2003. Cercopithecidae from Lothagam. In: Leakey,
778 M.G., Harris, J.M. (Eds.), Lothagam The Dawn of Humanity in Eastern Africa. Columbia University
779 Press, New York, pp. 201–248.
780
781 Leakey, M.G., 2007. Colobinae (Mammalia, Primates) from the Omo Valley, Ethiopia. In:
782 Coppens, Y., Clark Howell, F. (Eds.), Les Faunes Plio-Pleistocenes de la Basse Vallée de l'Omo
783 (Ethiopie), Tome 3: Cercopithecidae de la Formation de Shungura. Editions du CNRS, Paris, pp.
784 148–169.
785
786 Lebatard, A.-E., Bourlès, D.L., Braucher, R., Arnold, M., Duringer, P., Jolivet, M., Moussa, A.,
787 Deschamps, P., Roquin, C., Carcaillet, J., Schuster, M., Lihoreau, F., Likius, A., Mackaye, H.T.,
788 Vignaud, P., Brunet, M., 2010. Application of the authigenic 10Be/9Be dating method to
789 continental sediments: Reconstruction of the Mio-Pleistocene sedimentary sequence in the
790 early hominid fossiliferous areas of the northern Chad Basin. Earth and Planetary Science
791 Letters. 297, 57–70.
792
793 McKee, J.K., von Mayer, A., Kuykendall, K.L., 2011. New species of *Cercopithecoides* from

794 Haasgat, North West Province, South Africa. Journal of Human Evolution. 60, 83–93.
795
796 Merceron, G., Scott, J., Scott, R.S., Geraads, D., Spassov, N., Ungar, P.S., 2009. Folivory or
797 fruit/seed predation for *Mesopithecus*, an earliest colobine from the late Miocene of Eurasia?
798 Journal of Human Evolution. 57, 732–738.
799
800 Nakatsukasa, M., 1994. Morphology of the humerus and femur in African mangabeys and
801 guenons: functional adaptation and implications for the evolution of positional behavior. African
802 Study Monographs. 1–61.
803
804 Nakatsukasa, M., Mbua, E., Sawada, Y., Sakai, T., Nakaya, H., Yano, W., Kunimatsu, Y., 2010.
805 Earliest colobine skeletons from Nakali, Kenya. American Journal of Physical Anthropology. 143,
806 365–382.
807
808 Pan, R., 2006. Dental morphometric variation between African and Asian colobines, with special
809 reference to the other Old World monkeys. Journal of Morphology. 267, 1087–1098.
810
811 Patel, B.A., Ruff, C.B., Simons, E.L.R., Organ, J.M., 2013. Humeral cross-sectional shape in
812 suspensory primates and sloths: Long bone cross-sectional shape. The Anatomical Record. 296,
813 545–556.
814
815 Rafferty, K.L., 1998. Structural design of the femoral neck in primates. Journal of Human

816 Evolution. 34, 361–383.
817
818 Rose, M.D., 1988. Another look at the anthropoid elbow. Journal of Human Evolution. 17, 193–
819 224.
820
821 Ross, C.F., Iriarte-Diaz, J., Nunn, C.L., 2012. Innovative approaches to the relationship between
822 diet and mandibular morphology in primates. International Journal of Primatology. 33, 632–660.
823
824 Rossie, J.B., Gilbert, C.C., Hill, A., 2013. Early cercopithecid monkeys from the Tugen Hills, Kenya.
825 Proceedings of the National Academy of Sciences. 110, 5818–5822.
826
827 Schuster, M., 2006. The Age of the Sahara Desert. Science. 311, 821–821.
828
829 Suwa, G., Beyene, Y., Nakaya, H., Bernor, R.L., Boisserie, J.-R., Bibi, F., Ambrose, S.H., Sano, K.,
830 Katoh, S., Asfaw, B., 2015. Newly discovered cercopithecid, equid and other mammalian fossils
831 from the Chorora Formation, Ethiopia. Anthropological Science. 123, 19–39.
832
833 Swindler, D.R., Orlosky, F.J., 1974. Metric and morphological variability in the dentition of
834 colobine monkeys. Journal of Human Evolution. 3, 135–160.
835
836 Szalay, F.S., Delson, E., 1979. Evolutionary history of the primates, Academic Press, New York.
837

838 Thiery, G., Gillet, G., Lazzari, V., Merceron, G., Guy, F., 2017. Was *Mesopithecus* a seed eating
839 colobine? Assessment of cracking, grinding and shearing ability using dental topography. Journal
840 of Human Evolution. 112, 79–92.
841
842 Ting, N., 2008. Mitochondrial relationships and divergence dates of the African colobines:
843 evidence of Miocene origins for the living colobus monkeys. Journal of Human Evolution. 55,
844 312–325.
845
846 Williams, F.L., Geissler, E., 2014. Reconstructing the diet and paleoecology of Pli-Pleistocene
847 *Cercopithecoides williamsi* from Sterkfontein, South Africa. PALAIOS. 29, 483–494.
848
849 Youlatos, D., Koufos, G.D., 2010. Locomotor evolution of Mesopithecus (Primates: Colobinae)
850 from Greece: evidence from selected astragalar characters. Primates. 51, 23–35.
851
852 Youlatos, D., Couette, S., Koufos, G.D., 2012. A functional multivariate analysis of *Mesopithecus*
853 (Primates: Colobinae) humeri from the Turolian of Greece. Journal of Human Evolution. 63, 219–
854 230.
855
856
857 **Figure captions**
858 Figure 1. Dental indices of *C. bruneti* holotype (TM 266 03-100) and extinct African colobines.
859 Morphologies of extant cercopithecids associated with the maximum and minimum ratio value

860 are figured on the right of the graphs. Violin plots of extant Colobini on the right. Boxplots of
861 early colobines on the left. Miocene colobines in underlined brown font and boxplot in brown
862 background. Plio-Pleistocene colobine boxplots in grey background. Boxplots with mean (red
863 circle), median (black square), first quartile, third quartile, minimum and maximal values as well
864 as outliers (red diamonds). *C. bruneti* values identified by a black arrow. ASBI: As Sahabi;
865 LMDG'O: Lemudong'o; MNCR: Menacer; KF: Koobi Fora; EA: East Africa; SA: South Africa. Dental
866 indices calculated from value provided in Freedman, 1957; Delson, 1973; Frost, 2001; Frost et
867 al., 2003, 2014; Leakey et al., 2003; Leakey, 1987; Hlusko, 2006, 2007; Benefit et al., 2008;
868 Gilbert and Frost, 2008; Jablonski and Leakey, 2008; Suwa et al., 2015.
869 **(*A.*)** M^2 crown shape ratio (CSR) as M^2 PBL*100/MD with *Colobus* sspp. (*n*=50), *Piliocolobus* sspp.
870 (*n*=16), *Procolobus verus* (*n*=12) and African fossil colobines. **(*B.*)** P^{3-4} breadth differential (BD) as
871 P^3BL*100/P^4BL with *Colobus* sspp. (*n*=45), *Piliocolobus* sspp. (*n*=16), *Procolobus verus* (*n*=12) and
872 African fossil colobines **(*C.*)** Boxplot of the upper molars NH/NR ratio of *C. bruneti* (*n*=1; M^2 from
873 TM 266 03-100), *C. williamsi* (*n*=1; M^1 from KB5277), *M. pentelicus* (*n*=3; M^2 from NHMW 1863,
874 NHMW 1998, PK25), M^2s from extant Cercopithecinae (*n*=8) and extant Colobinae (*n*=18).
875
876 Figure 2. Digital photographs of *C. bruneti* maxillary remains. ***A.-N.*** TM 266 03-100 (***A.-F.***) left
877 side, (***G.-L.***) right side, (***B.&G.***) mesial view, (***A.&H.***) distal view, (***C.&J.***) buccal view, (***D.&I.***)
878 lingual view, (***E.&L.***) superior view, (***F.&K.***) occlusal view, (***M.***) section at the mesial loph of right
879 M^2, (***N.***) section at the mesial loph of left M^2 (***N.***). ***O.-Z.*** TM 266 03-034 (***Q.&Z.***) lingual view,
880 (***O.&V.***) mesial view, (***P.&Q.***) buccal view, (***R.&Y.***) occlusal view, (***S.&X.***) labial view, (***T.&W.***)
881 lingual view.

882 Abbreviations: A= Anterior; Ap= Apical; M= Medial, P= Posterior, L= Lateral, B= Buccal, M=
883 Medial, S= Superior.
884
885 Figure 3. ***(A.)*** Comparative anatomy of *Cercopithecoides spp.* (i.e., *C. bruneti* and *C. williamsi*)
886 dental morphology relative to extant Colobini (i.e., *Colobus spp.*, *Piliocolobus spp.* and
887 *Procolobus verus*). ***(B.)*** Comparative anatomy of juvenile *Cercopithecoides* spp. (i.e., *C. bruneti*
888 and *C. williamsi*) cranial morphology relative to extant juvenile Colobini (i.e., *Colobus guereza*
889 sspp. indet.) with photographs courtesy of the Mammalian Crania Photographic Archive Second
890 Edition (MCPA2) of the Dokkyo Medial University
891 (http://1kai.dokkyomed.ac.jp/mammal/en/mammal.html).
892 Abbreviations: Mes=Mesial, Lng=Lingual, Sup=: Superior, Lat=Lateral, Post=Posterior,
893 Ant=Anterior.
894
895 Figure 4. Digital photographs of C*. bruneti* mandibular remains. ***A.-I.*** TM 219 01-102 ***(A.)*** occlusal
896 view, ***(B.)*** inferior view, ***(C.)*** right side view, ***(D.)*** left side view, ***(E.)*** labial view, ***(F.)*** posterior
897 view, (***G.***) sagittal cross-section at symphysis, (***H.***) coronal cross-section at mid-P_3 a, ***(I.)***. coronal
898 cross-section mid-M_2. ***J.-R.*** TM 266 03-099 ***(J.)*** occlusal view, ***(L.)*** inferior view, ***(M.)*** right side
899 view, ***(N.)*** labial view, ***(E.)*** labial view, ***(O.)*** posterior view (***P.***) sagittal cross-section at symphysis
900 (***Q.***) coronal cross-section at mid-P_3, (***R.***) coronal cross sectionsand mid-M_1. ***S.-A3.*** TM 112 00-
901 093 (***Y.***) sagittal cross-section at symphysis, (***Z.***) coronal cross-sections at mid-P_3, (***A1.***) coronal
902 cross-section at mid-M_1, (***A2.***) coronal cross-section at mid-M_2 , (***A3.***) coronal cross-section at
903 mid-M_3.

904 Abbreviations: S= Superior; A=Anterior; M=Medial, P=Posterior, L=Lateral.

905

906 Figure 5. Comparative anatomy of *Cercopithecoides spp.* (i.e., *C. bruneti* and *C. williamsi*)
907 mandibular morphology relative to extant Colobini (i.e., *Colobus guereza occidentalis*,
908 *Piliocolobus badius badius* and *Procolobus verus*). ***A.1-3*** anterior view, ***B.1-3*** lateral view, ***C.1-3***
909 superior view, ***D.1-3*** saggital cross-section at symphysis, ***E.1-3*** coronal cross-section at mid-M_1.
910 Abbreviations: Sup=Superior, Lat=Lateral, Post= Posterior, Ant= Anterior.

911

912 Figure 6. Mandibular morphometric indices of *C. bruneti* paratypes (i.e., TM 266 03-099, TM 219
913 01-102, TM 112 00-093), *C. williamsi* (i.e., KB680, STS 394) and extant African (*n*=37) and Asian
914 colobines (*n*=66). Morphologies of extant Colobinae associated with the maximum and
915 minimum ratio value are figured on the right of the graphs. Violin plots of extant Colobini and
916 Presbytini on the right. Boxplots of early colobines on the left. Miocene colobines in underlined
917 brown font and boxplot in brown background. Plio-Pleistocene colobine boxplots in grey
918 background. Boxplots with mean (red circle), median (black line), first quartile, third quartile,
919 minimum and maximal values as well as outliers (red diamonds). *C. bruneti* values identified by
920 a black arrow. For extended measurement protocol, refer to SOM Figure S1. **(*A.*)** STT/ITT ratio of
921 *C. bruneti* (*n*=3), *C. williamsi* (*n*=1; KB680) and extant African and Asian Colobinae with STT/ITT
922 as [(SBSTT/SBITT)*100]. **(*B.*)** Symphyseal angle of *C. bruneti* (*n*=3), *C. williamsi* (*n*=1; KB680) and
923 extant African and Asian Colobinae. ***(C.)*** Relative position of the genioglossal fossa (GFP) of *C.*
924 *bruneti* (*n*=2; TM 219 01-102, TM 112 00-093), *C. williamsi* (*n*=1; KB680) and extant African and
925 Asian Colobinae with GFP as [(GFH/SL)*100]. **(*D.*)** Symphyseal robustness (SR) in *C. bruneti* (*n*=3;

926 TM 266 03-099, TM 219 01-102, TM 112 00-093), *C. williamsi* (*n*=1; KB680) and extant African
927 and Asian Colobinae with SR as [(SB/SL)*100]. ***(E.)*** Planum alveolare extension (PAE) in *C.*
928 *bruneti* (*n*=3), *C. williamsi* (n=1; KB 680) and extant African and Asian Colobinae with PAE as
929 [(PAL/SL)*100]. ***(F.)*** Corpus robustness (CR) at M_1 in *C. bruneti* (*n*=2; TM 266 03-099, TM 112 00-
930 093), *C. williamsi* (*n*=2; KB 680, STS 394) and extant African and Asian Colobinae with CR as
931 [(CWM1/CLM1)*100].
932
933 Figure 7. Digital photographs of *C. bruneti* postcranial remains (i.e., TM 266 03-100 and TM 266
934 03-307) with *C. bruneti* ulna ***(A.-D.)***, radius ***(E.-H.)***, humerus ***(I.-L.)*** and femur ***(M.-P.)***.
935 Abbreviations: Px=Proximal; A= Anterior; M= Medial, P= Posterior, L= Lateral.
936
937 Figure 8. Comparative anatomy of extant and extinct Colobinae forelimbs. ***(A.)*** *C. guereza*
938 *guereza.* ***(B.)*** *P. rufomitratus langi*. ***(C.)*** *M. pentelicus*. ***(D.)*** *Microcolobus.* sp. with photographs
939 reproduced from (Nakatsukasa et al., 2010)). ***(E.)*** Forelimb anatomy of *C. bruneti*. Abbreviations:
940 Prox= Proximal; Med= Medial, Post= Posterior, Lat=Lateral.
941
942 Figure 9. Postcranial indices of extant cercopithecids, *C. bruneti* and early colobines (i.e.,
943 *Mesopithecus pentelicus*). Morphologies of extant cercopithecids associated with the maximum
944 and minimum ratio value are figured on the right of the graphs. Violin plots of extant
945 cercopithecids on the right. Boxplots of early colobines on the left. Miocene colobines in
946 underlined brown font and boxplot in brown background. Boxplots with mean (red circle),
947 median (black square), first quartile, third quartile, minimum and maximal values as well as

948 outliers (red diamonds). *C. bruneti* values identified by a black arrow. For extended
949 measurement protocol of medial epicondyle angulation, refer to SOM Figure S1.
950 **(*A.*)** Boxplot of the medial epicondyle angulation of *C. bruneti* (n=1; TM 266 03-036), *M.*
951 *pentelicus* (*n*=6; PIK 244, 245, 355, 356, 1429, 1727), extant *Papio* ssp. (*n*=26), extant Colobini
952 (*n*=44) and extant Presbytini (*n*=38). **(*B.*)** Boxplot of the medial trochlear keel relative
953 development of *C. bruneti* (*n*=1; TM 266 03-036), *C. williamsi* (*n*=1; KNM-ER 4420 with data from
954 Frost and Delson, 2002), *C. meavae* (*n*=1; AL2-64 with data from Frost and Delson, 2002), *M.*
955 *pentelicus* (*n*=7; PIK 244, 245, 355, 356,1727,1728,1729), extant *Papio* ssp. (*n*=17), extant
956 Colobini (*n*=34) and extant Presbytini (*n*=22). Medial trochlear keel development calculated and
957 measured as in (Frost and Delson, 2002). **(*C.*)** Boxplot of the Imax/Imin ratio of *C. bruneti* (*n*=1;
958 TM 266 03-034), extant cercopithecines (*n*=6) and extant colobines (*n*=17).
959

A.
M2 CSR
120
110
100
90
80
Procolobus verus sp.
Piliocolobus sspp.
Colobus sspp.
WM colobine sp. B
R. turkaenensis KF
P. mutiwa KF
P. chemeroni
P. enkorikae
Nawata colobine sp. B
MNGR putative colobine
L. markgrafi
LMDG 'O small colobine
K. hafu
K. aramisi
K. aramisi Asbole
Colobus sp.
Colobus freedmani
Colobus cf. angolensis
C. williamsi SA
C. williamsi EA
C. meaveae
C. cf. meaveae
C. kimeui
C. harenna
C. alemayehui
C. brunneti
Beticha colobine
ASBI putative colobine
B.
P3-4 BD
110
100
90
80
70
Procolobus sp.
Piliocolobus sspp.
Colobus sspp.
WM colobine sp. B
R. turkaenensis Omo
P. mutiwa KF
R. turkaenensis
P. chemeroni
P. enkorikae
L. markgrafi
LMDG 'O small colobine
K. hafu
K. aramisi
K. aramisi Asbole
Colobus sp.
Colobus freedmani
Colobus cf. angolensis
C. williamsi SA
C. williamsi EA
C. meaveae
C. kimeui
C. harenna
C. alemayehui
C. brunneti
C.
NH/NR
160
120
80
40
Extant Colobinae
Extant Cercopithecinae
M. pentelicus
C. williamsi
C. brunneti

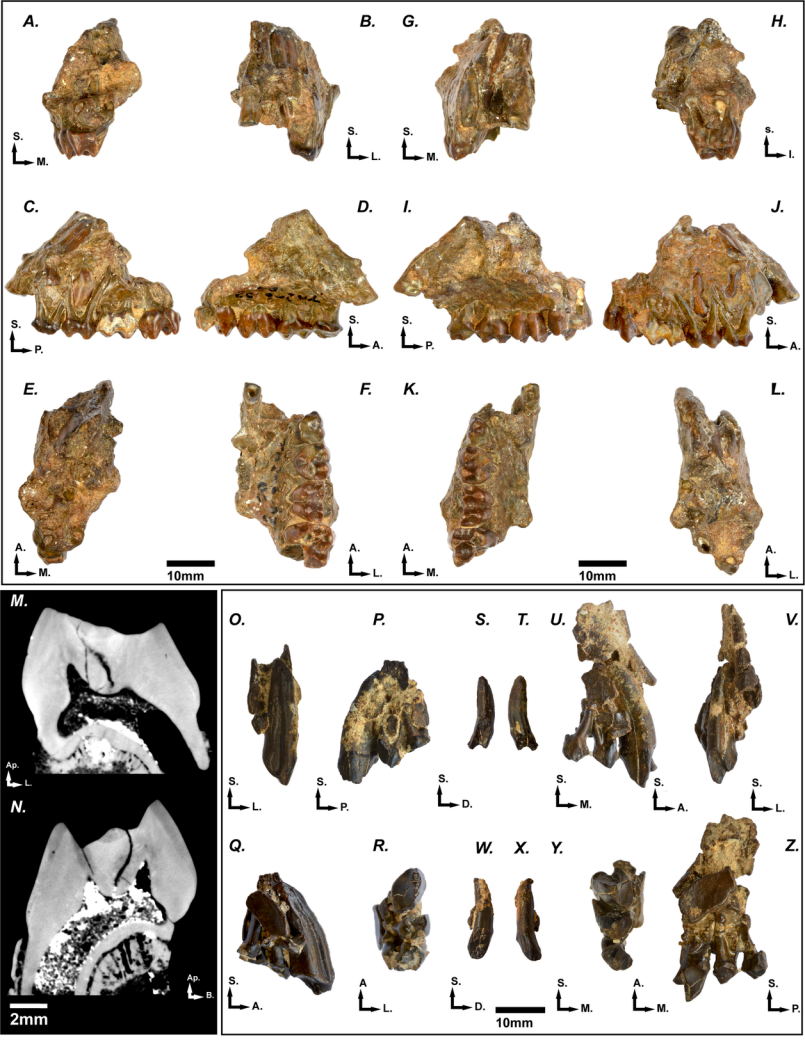
A.
B.
G.
H.
C.
D.
I.
J.
E.
F.
K.
L.
S.
M.
L.
I.
P.
A.
10mm
M.
Ap.
N.
B.
2mm
O.
P.
S.
T.
U.
V.
Q.
R.
W.
X.
Y.
Z.
D.

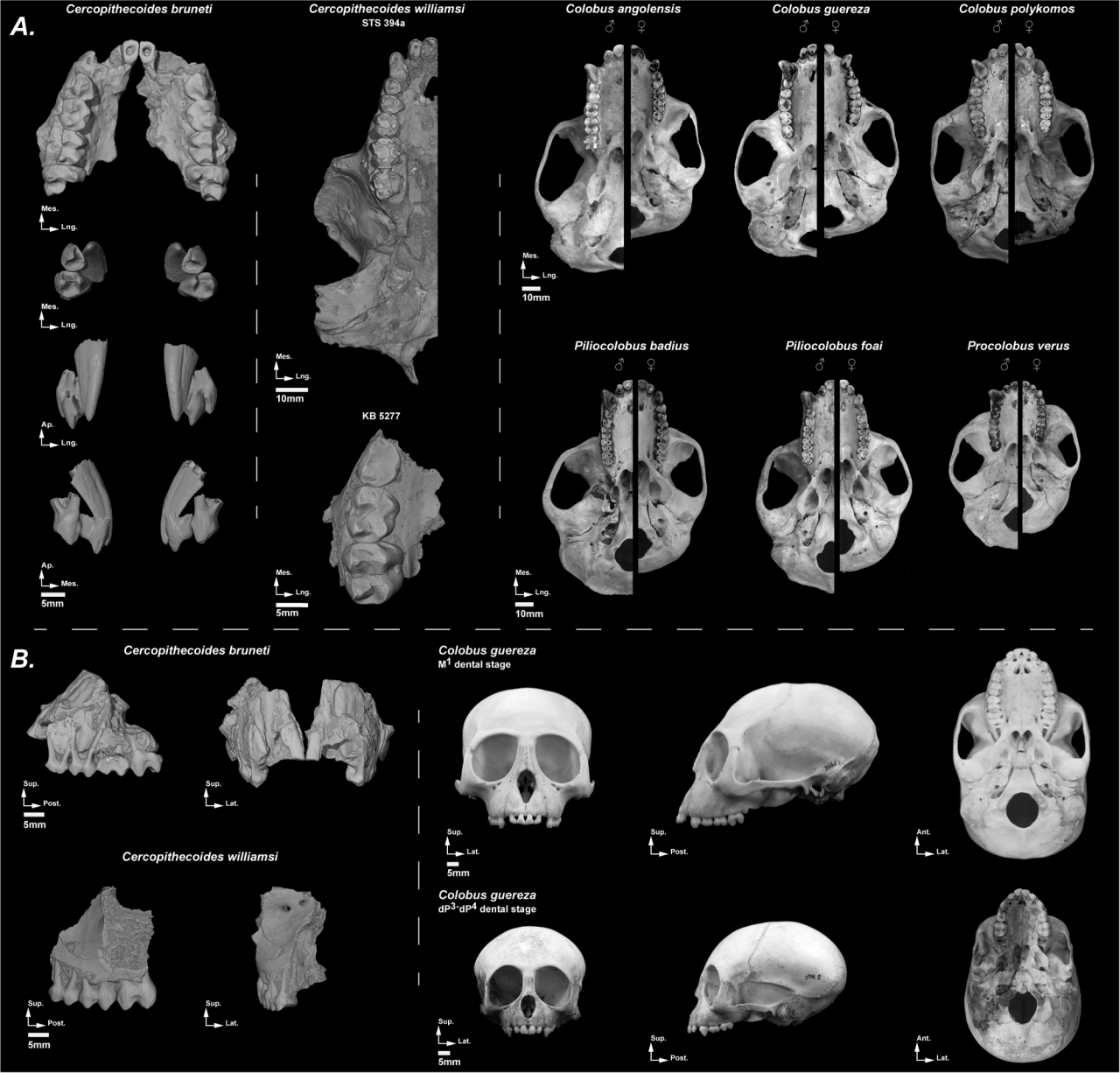
A.
Cercopithecoides bruneti
Cercopithecoides williamsi
STS 394a
KB 5277
Colobus angolensis
Colobus guereza
Colobus polykomos
Piliocolobus badius
Piliocolobus foai
Procolobus verus
♂
♀
Mes.
Lng.
Ap.
10mm
5mm
B.
Cercopithecoides bruneti
Cercopithecoides williamsi
Colobus guereza
M1 dental stage
Colobus guereza
dP3-dP4 dental stage
Sup.
Post.
Lat.
Ant.

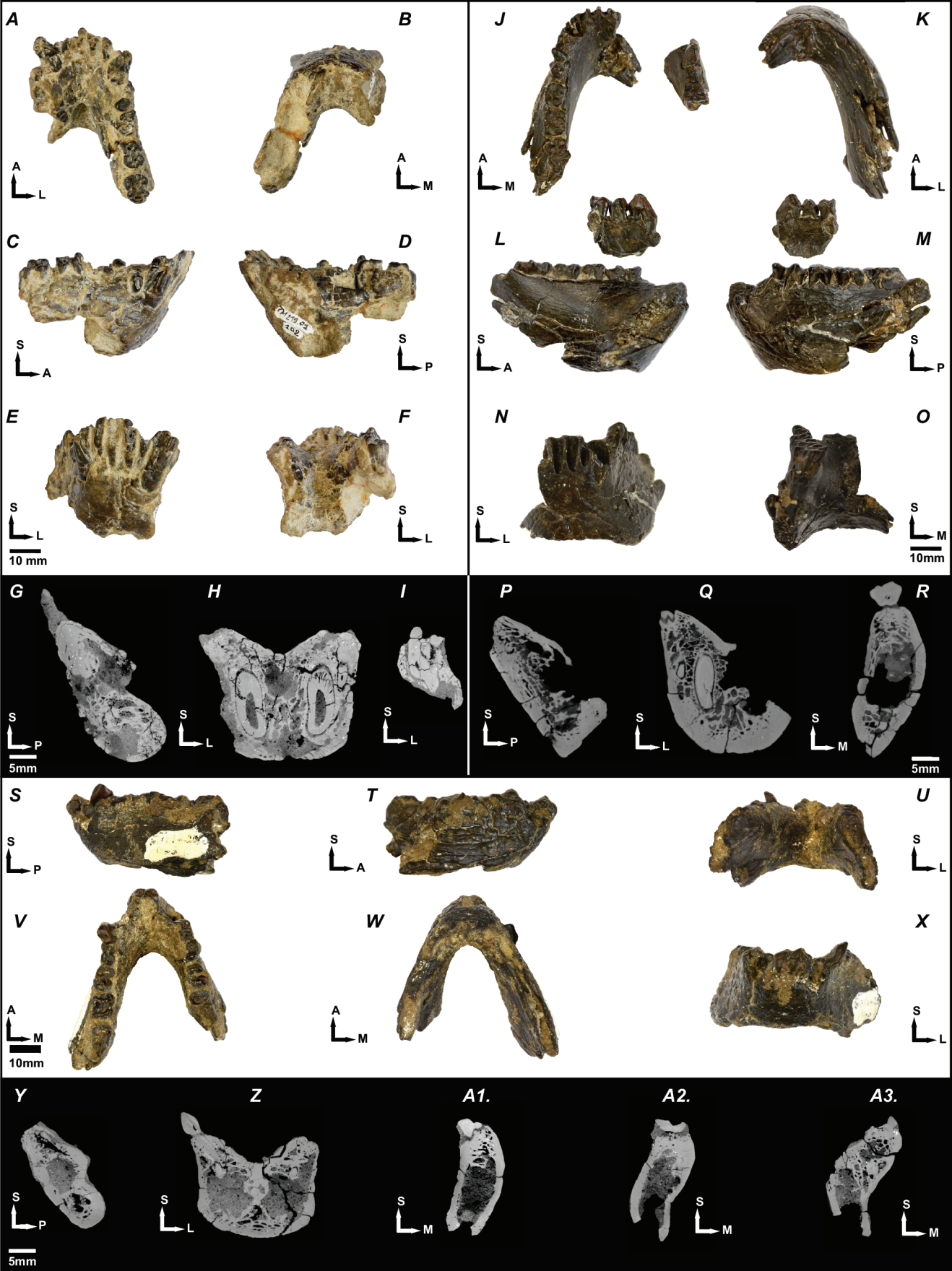
A
A
L
B
A
M
J
A
M
K
A
L
C
S
A
D
S
P
L
S
A
M
S
P
E
S
L
F
S
L
N
S
L
O
S
M
10 mm
10mm
G
S
P
H
S
L
I
S
L
P
S
P
Q
S
L
R
S
M
5mm
5mm
S
S
P
T
S
A
U
S
L
V
A
M
10mm
W
A
M
X
S
L
Y
S
P
Z
S
L
A1.
S
M
A2.
S
M
A3.
S
M
5mm

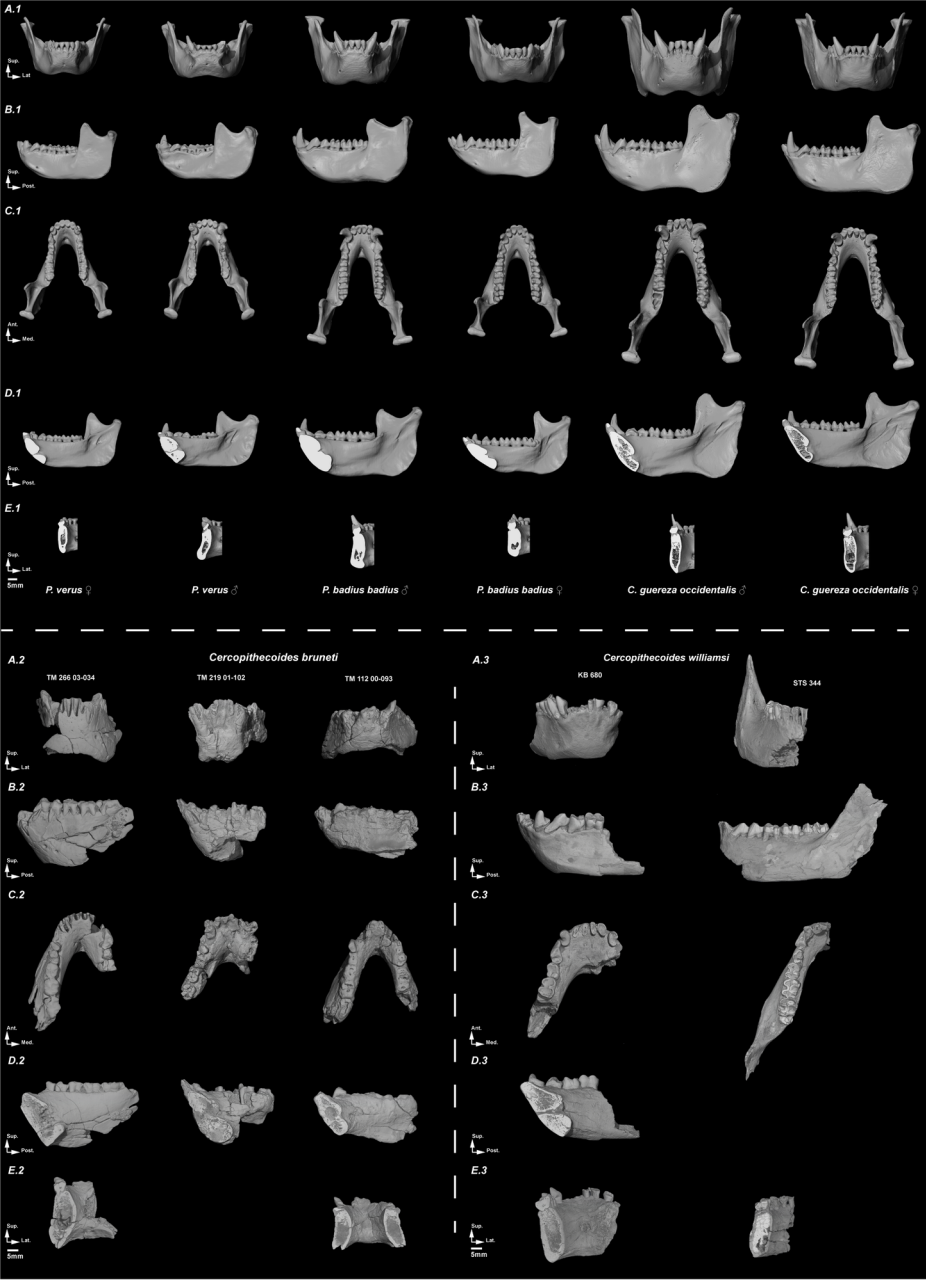
A.1
Sup.
Lat.
B.1
Sup.
Post.
C.1
Ant.
Med.
D.1
Sup.
Post.
E.1
Sup.
Lat.
5mm
P. verus ♀
P. verus ♂
P. badius badius ♂
P. badius badius ♀
C. guereza occidentalis ♂
C. guereza occidentalis ♀
Cercopithecoides bruneti
TM 266 03-034
TM 219 01-102
TM 112 00-093
A.2
B.2
C.2
D.2
E.2
Cercopithecoides williamsi
KB 680
STS 344
A.3
B.3
C.3
D.3
E.3

A.
STT/ITT
B.
SA (°)
C.
GFP
D.
SR
E.
PAE
F.
CR
Presbytini
Colobini
Trachypithecus ssp.
Simias concolor
Semnopithecus roxellana
Rhinopithecus ssp.
Pygathrix ssp.
Procolobus verus
Presbytis ssp.
Pilocolobus ssp.
Nasalis larvatus
Colobus ssp.
C.williamsi
C.brunneti


A.
B.
Px.
P.
Px.
A.
C.
D.
Px.
L.
Px.
M.
20mm
E.
F.
Px.
P.
Px.
A.
G.
H.
Px.
L.
Px.
M.
20mm
I.
J.
Px.
L.
Px.
A.
K.
L.
Px.
P.
Px.
M.
20mm
M.
N.
Px.
L.
Px.
P.
O.
P.
Px.
A.
Px.
M.
20mm

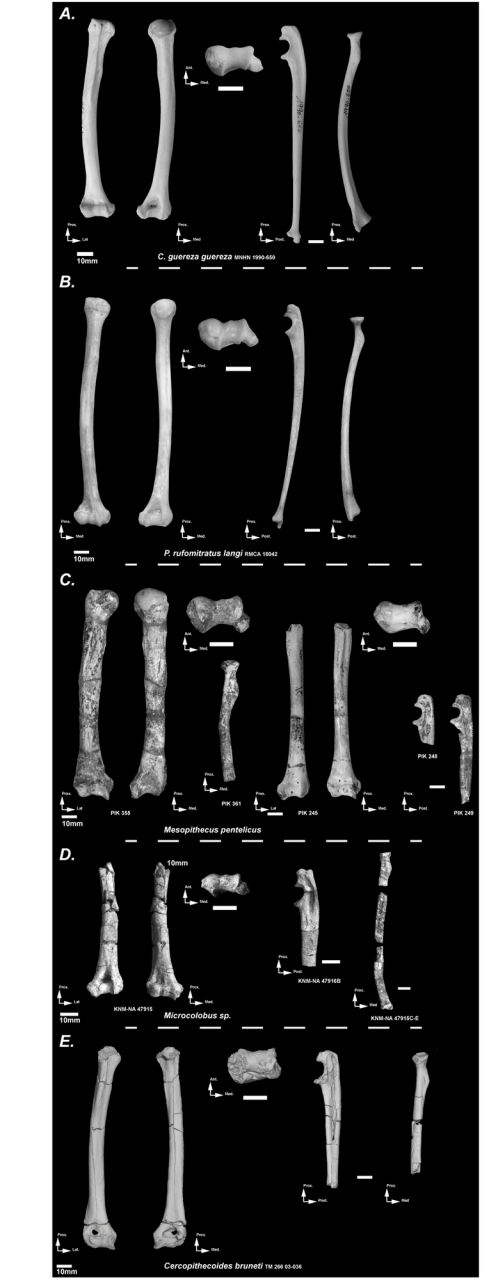
A.
Ant.
Med.
Prox.
Lat.
Prox.
Med.
Prox.
Post.
Prox.
Med.
10mm
C. guereza guereza MNHN 1990-650
B.
Ant.
Med.
Prox.
Med.
Prox.
Post.
Prox.
Post.
10mm
P. rufomitratus langi RMCA 19942
C.
Ant.
Med.
Ant.
Med.
PIK 248
Prox.
Lat.
Prox.
Med.
Prox.
Lat.
Prox.
Med.
Prox.
Post.
10mm
PIK 355
PIK 361
PIK 245
PIK 249
Mesopithecus pentelicus
D.
10mm
Ant.
Med.
Prox.
Post.
Prox.
Lat.
Prox.
Med.
Prox.
Med.
10mm
KNM-NA 47915
KNM-NA 47916B
KNM-NA 47915C-E
Microcolobus sp.
E.
Ant.
Med.
Prox.
Post.
Prox.
Post.
Prox.
Lat.
Prox.
Med.
10mm
Cercopithecoides bruneti TM 266 03-036

A.
Medial epicondyle angulation (°)
70
60
50
40
30
20
Papio sp.
Presbytini
Colobini
Mesopithecus pentelicus
Cercopithecoides bruneti
B.
Medial trochlear keel relative development
80
70
60
50
40
Presbytini
Papio sp.
Colobini
Mesopithecus pentelicus
Cercopithecoides bruneti
Cercopithecoides williamsi
Cercopithecoides meavae
C.
lmax/lmin
2.0
1.5
1.0
Colobinae
Cercopithecinae
Cercopithecoides bruneti

Table 1: Spatial and temporal setting of the *Cercopithecoides* representatives

	Type locality	***Temporal record***	***Spatial record***
C. bruneti	Toros-Menalla, Chad, **Central Africa**.	ca. 7 Ma.	Only known from its type locality.
C. kerioensis	Lothagam, Kenya, **East Africa**.	ca. 5-4.2 Ma.[1]	Only known from its type locality.
C. meavae	Leadu, Ethiopia, **East Africa**.	3.8 - 3.28 Ma.[2]	Hadar, Leadu, Woranso-Mille[2].
C. kimeui	Olduvai Gorge, Tanzania, **East Africa**	2.5-1.2 Ma.	Olduvai Gorge, Rawi, Koobi Fora, Hadar.
C. haasgati	Haasgat, **South Africa**.	?Pleistocene.[3]	Only known from its type locality.
C. williamsi	Makapansgat, **South Africa**.	3.5-1.5 Ma.	Makapansgat, Sterkfontein, Swarktrans, Cooper's A, Bolt's Farm, Kromdraai, Drimolen, Koobi Fora, ?Shungura, Leba (Angola).
C. alemayehui	Daka, Ethiopia, **East Africa**.	1.0 Ma.	Only known from its type locality.
C. sp. indet. Laetoli	Laetoli, Tanzania, **East Africa**.	3.81-3.63 Ma.	Uncertain taxonomy and known only from Laetoli.
cf. *C. sp. indet.* Koobi Fora	Koobi Fora, Ethiopia, **East Africa**.	3.95-3.45 Ma.	Uncertain taxonomy and known only from Allia Bay[4].
i C. sp. indet. Kanapoi	Kanapoi, Kenya, **East Africa**	4.19-4.11 Ma.	Uncertain taxonomy and known only from Kanapoi.

[1] According to Leakey et al., 2003, there is no secure stratigraphic context relative to *C. kerioensis*.

[2] It includes here specimens from Woranso-Mille and allocated to *C. cf. meavae*.

[3] According to McKee et al., 2011, there is uncertainty relative to the exact temporal setting of the *Cercopithecoides* sample from Haasgat

[4] According to Jablonski et al., 2008, a partial mandible, KNM-ER 36985, exhibit phenetic affinities with *C. kerioensis* but the authors referred to this specimen as *C. sp. indet.*

[5] Uncertain age estimation based on faunal assemblage (Jablonski, 1994)

Table 2: Comparative morphology of the cranio-dental anatomy of *Cercopithecoides spp.*

	BM (kg)[1]	M^2 CSR	P^3-P^4 BD	P^3 protocone	M_3 RHD	M_{1-2} SD	P_4 CSR	MS	STT/ITT	CW
C. bruneti	16.6 - 8.4	111.5	77.2	Faint	63.2	75.4	73	Present	127.6 - 104.3	39.9 - 39.3
C. kerioensis	9.8[2]	NA	93.9	Faint	62.5	NA	NA	NA	NA	NA
C. meavae	17.7 – 15.0[3]	100.0 - 98.9	89.5	Faint	69.5 – 58.2	87.5 - 75.3	74.2 - 61.2	NA	NA	NA
C. kimeui	51.0 - 25.0[4]	106.4 - 89.4	89.2 – 84.0	Faint	89.2 - 84	88.7	76.1	Present	NA	NA
C. williamsi	23.0 – 16.0[4]	107.4 - 87.5	84.8 - 73.1	Faint	84.8 – 73.1	87.6 - 70.9	101.6 - 78.6	Present	142.4	53.2 - 41.1
C. alemayehui	16.3[5]	100.0	82.6	Faint	NA	NA	NA	?Present[8]	NA	NA
C. haasgati	18.2 - 12.3[6]	107.2[7]	82.4[7]	Faint	69.4[7]	71.7[7]	96.6[7]	NA	NA	NA

Range values of odontometric indices and qualitative assessment of several morphological characteristics of *Cercopithecoides spp*. With Body Mass (BM); Crown Shape Ratio (CSR); Breadth Differential (BD); Relative Hypolophid Development (RHD); Maxillary Sinuses (MS); Superior Transverse Torus (STT); Inferior Transverse Torus (ITT); Corpus Width (CW); Not Available (NA).

[1] Based on the equation provided by Delson et al., 2000.

[2] Calculated from M^1 MD dimension with *"All-colobine"* model parameters.

[3] Range value calculated from M^2 MD dimension with *"All-colobine"* model parameters.

[4] Values given in Delson et al., 2000 for the *"Estimated mass"* value.

[5] Calculated from M^2 MD dimension with *"All-colobine"* model parameters.

[6] Range value alculated from M^2 MD dimension with *"All-colobine"* model parameters on minimum and maximum dental dimensions provided in McKee et al., 2011.

[7] Ratio calculated from mean dental dimensions provided in McKee et al., 2011.

[8] The presence of MS is not clearly asserted (Frost et al., 2008).

Table 3 : *C. bruneti* holotype (i.e TM 266 03-100) dental metrics

Measurements

dP^3 MD^1	**5.6 (5.5)**	P^3 MD^2	**6.0 (5.9)**
dP^3 BL^1	**5.4 (5.3)**	P^3 BL^2	**6.1 (6.1)**
dP^4 MD^1	**7.1 (6.8)**	P^4 MD^2	**6.0 (6.1)**
dP^4 PBL^1	**6.8 (6.8)**	P^4 BL^2	**7.8 (7.9)**
dP^4 MBL^1	**6.6 (6.3)**	M^1 MD^1	**7.5 (7.8)**
C^1 MD^2	**8.4 (8.6)**	M^2 MD^1	**8.3**
C^1 BL^2	**5.2 (5.3)**	M^2 MBL^1	**9.4**

Dental metrics in mm and dental metrics of right teeth given in brackets. *MD*: mesio-distal dimension; *BL*: bucco-lingual dimension; *MBL:* bucco-lingual dimension at the paraloph. Measurement protocol from (Benefit, 1993).
Extended dental metrics in Table S2.
[1] Measurements acquired using a *Mitutoyo* Digital Calliper CD-8''CX on original specimens
[2] Measurements acquired on ImageJ through selected photographs of the segmented model obtained in Avizo Standard Edition

Table 4: Dental metrics and dental indices of *C. bruneti* lower dentition (i.e TM 266 03-099; TM 112 00-093; TM 219 01-102)

Measurement	TM 266 03-099	TM 112 00-093	TM 219 01-102
C_1 MD	~5.4	~4.3 (~4.4)	6.7
C_1 BL	~8.5	~5.2 (~5.3)	8.9 (9.1)
P_3 OL	(7.6)	4.8	
P_3 TL	(10.2)	6.8	9.4
P_3 FL	(7.7)	6.3	
P_3 BL	(4.2)	3.2	
P_4 MD	6.1	5.5	6.3
P_4 BL	4.4		
M_1 MD	6.9	6.6	7.5
M_1 MBL	5.7		
M_1 HBL	5.6		
M_2 MD	7.7	7.1	7.9
M_2 MBL	6.8		
M_2 HBL	6.4		
M_3 MD	10.3	8.8	
M_3 HBL	6.5		
M_3 HYPOB	3.1		
M_3 HYPOB/HBL	47.9		
M_3 HBL/MD	63.4		
P_4 BL/MD	73.0		
M_{1-2} SD	75.5		
P_3 BL/OL	55.2	65.8	

Dental metrics in mm and right teeth metrics given in brackets. Dental indices and measurement protocols from (Benefit, 1993; Harrison and Harris, 1996). All measurements acquired using a *Mitutoyo* Digital Calliper CD-8''CX on original specimens. *MD*: mesio-distal dimension; *BL*: bucco-lingual dimension; *OL:* Occlusal length; *TL:* Total length; *FL*: Flange length as in (Benefit, 1993); *MBL:* bucco-lingual dimension at the metalophid; *HBL:* bucco-lingual dimension at the hypolophid; *HYPOB:* bucco-lingual dimension at the hypoconulid.

Table 5: Mandibular morphometry of *C. bruneti* hypodigm

	TM 266 03-099	TM 112 00-093	TM 219 01-102
SL	26.7	20.8	27.5
SA	63.4	62	62.6
GFH		7.9	27.5
PAL	11.3	11.3	27.5
SB	12.3	9.7	27.5
SBSTT	11.3	9.7	27.5
SBITT	12.3	7.6	27.5
CWM1	26.7	18.8	27.5
CLM1	10.5	7.5	27.5

Morphometric data in mm. All measurements taken on selected photographs of symphyseal and corporeal cross section obtained through Avizo and Geomagic and measured through ImageJ. *SL*: symphyseal length; *SA*: symphyseal angle; *GFH:* genioglossal fossa height; *PAL*: planum alveolare length; *SB*: maximum breadth of the symphysis; *SBSTT*: breadth of the symphysis at the STT (superior transverse torus) level; *SBITT*: breadth of the symphysis at the ITT (inferior transverse torus) level; *CWM*1: corpus width at mid-M_1; *CLM1*: corpus length at mid-M_1. For an extended description of the morphometric protocol, refers to SOM Figure S1.

Table 6: *C. bruneti* postcranial morphometric data

Measurements	
HTL	151.7
HML	10.6
HAP	11.7
HAW	19.7
MEPP	2.3
TW	7.0
HAH	11.0
MKPD	12.1
HCW	12.0
HDW	25.3
HDB	15.3
MEA[1]	50.1°
OPH	11.9
TNH	15.9
CPH[1]	7.5
TWMH	8.0
RHAP	14.4
RHML	11.0
RNAP	9.4
RNML	6.2
RTP	8.5
*FAP**	~14.1
*FML**	~14.8
*FNAP**	~10.0
*FNSI**	~11.8
*FNSA**[1]	124°

All measurements in mm and acquired using a *Mitutoyo* Digital Calliper CD-8''CX. *HTL*: Humeral total length; *HML*: Humeral medio-lateral diameter at mid-diaphysis (HTL+5%); *HAP*: Humeral antero-posterior diameter at mid-diaphysis (HTL+5%); *HAW*: Humeral articular width measured as in (Birchette, 1982); *MEPP*: Medial epicondyle posterior projection measured as in (Birchette, 1982); *TW*: Humeral trochlear width measured as in (Birchette, 1982); *HAH*: Humeral distal articular height measured as in (Birchette, 1982); *MKPD*: Humeral medial keel distal projection measured as in (Frost and Delson, 2002); *HCW*: Humeral capitulum and zona conoidea width measured as in (Birchette, 1982); *HDW*: Humeral distal epiphysis width measured as in (Harrison, 1989); *HDB*: Humeral distal epiphysis breadth measured as in (Rose, 1988); *MEA*: Medial epicondyle angulation as in the protocol presented in ;*OPH*: Ulnar olecranon process height measured as in (Ciochon, 1986); *TNH*=Ulnar trochlear notch height measured as in (Birchette, 1982); *CPH*: Ulnar coronoid process height measured as in (Birchette, 1982); *TWMH*: Ulnar trochlear width at mid-height measured as in (Birchette, 1982); *RHAP*: Radial head antero-posterior diameter measured as the long axis of the radial head; *RHML*: Radial head medio-lateral diameter measured as the short axis of the radial head; *RNAP*: Radial neck antero-posterior diameter measured as the long axis of the radial neck; *RNML*: Radial neck medio-lateral diameter as the short axis of the radial neck; *RTP*: Radial tuberosity projection measured as in (Birchette, 1982); *Due to conservation state, the measurement of TM 266 03-307 are given here as estimated value. *FAP*: Femoral mid-diaphysis antero-posterior diameter (taken as a rough estimate of the mid-diaphyseal point and diaphysis subject to distortion); *FML*: Femoral mid-diaphysis medio-lateral diameter (taken as a rough estimate of the mid-diaphyseal point and diaphysis subject to distortion); *FNAP*: Femoral neck antero-posterior diameter; *FNSI*: Femoral neck medio-lateral diameter (femoral neck superior portion abraded); *FNSA*: Femur neck-shaft angle.

[1] Measurements taken from selected photographs.